General Disclaimer

One or more of the Following Statements may affect this Document

- This document has been reproduced from the best copy furnished by the organizational source. It is being released in the interest of making available as much information as possible.

- This document may contain data, which exceeds the sheet parameters. It was furnished in this condition by the organizational source and is the best copy available.

- This document may contain tone-on-tone or color graphs, charts and/or pictures, which have been reproduced in black and white.

- This document is paginated as submitted by the original source.

- Portions of this document are not fully legible due to the historical nature of some of the material. However, it is the best reproduction available from the original submission.

NATIONAL AERONAUTICS AND SPACE ADMINISTRATION

THE CORRELATION OF RADAR SCATTEROMETER DATA WITH AERIAL TERRAIN PHOTOGRAPHY

CRES TECHNICAL REPORT 118-13

April 1969

Prepared by the University of Kansas Center for Research, Inc., Engineering Science Division, Lawrence, Kansas, for the National Aeronautics and Space Administration (NASA) under NASA Contract No. NAS 9-7175

MANNED SPACECRAFT CENTER

HOUSTON, TEXAS

CRES CENTER FOR RESEARCH, INC. · ENGINEERING SCIENCE DIVISION
THE UNIVERSITY OF KANSAS · LAWRENCE, KANSAS · 66044

THE CORRELATION OF RADAR SCATTEROMETER DATA WITH AERIAL TERRAIN PHOTOGRAPHY

by

J. M. Cullen
G. A. Bradley

CRES Technical Report 118-13

August 1968
(Revised March 1969)

The Remote Sensing Laboratory

Supported by NASA Contract No. NAS 9-7175

PREFACE

This report is intended to document early attempts to correlate and verify the relationship between measured scatterometry data and significant characteristics of the ground terrain. Because the report was initiated in the summer of 1968, it does not reflect recently proposed correlation improvements such as the spatially adjusted time history (SATH) plotting technique or the auxiliary data annotation system (ADAS) which promise to simplify the correlation procedure as well as improve the accuracy of the results.

THE CORRELATION OF RADAR SCATTEROMETER DATA WITH AERIAL TERRAIN PHOTOGRAPHY

J. M. Cullen
G. A. Bradley

Center for Research in Engineering Science
University of Kansas
Lawrence, Kansas 66044

ABSTRACT

This report presents a systematic method of correlating radar scatterometer data with aerial terrain photography. It is shown that the time base for the scatterometry data must be adjusted to correspond to that of the aerial photography in order to properly interpret and identify scattering coefficient signatures. Data are presented which show the correlation procedure for a section of Garden City, Kansas Mission 32. It is concluded that significant simplification of the data correlation procedure can be achieved by using common time synchronization for all future data recording and processing operations.

I. INTRODUCTION

The purpose of this report is to present a method of correlating radar scatterometer data with associated aerial terrain photography. Because one objective of the remote sensing program is to identify major characteristics of the earth using remote radar sensors, it is necessary to catalog scatterometry signature data for the various types of terrain. This catalog is compiled by correlating scatterometry data with photographs which detail the nature of the measured earth terrain.

A major problem in correlating electronic and visual data has been the lack of a unified time synchronization system for the several operations associated with data measurement and processing operations. In a typical run, the clock used for the measurement of electronic data is independent of the aerial camera clock. The method used for synchronization in Mission 32 involved photographing the master control panel digital clock each time an aerial photograph was taken. In interpreting the data, time correlation is required to line up the time base of the aerial photograph with the photograph of the scatterometer digital clock before a correlation can be made between electronic and photographic data. This interim step results in additional difficulty in preparing the data for analysis but the most significant disadvantage is the increased possibility of error resulting from lining up three separate but not independent information sources.

The problems involved with correlating the electronic and visual data can be further complicated if there is a difference in time scale between the photo mosaic of a given data run and the scatterometer data output of the digital computer processing program. If the time scales of these two records are different, the scatterometer data must be replotted on a time scale identical to that of the photo mosaic. To obviate this rescaling process, which must be performed by hand, a time scale identical to the photo time should be specified for the use in the digital processing readout.

This report shows the procedure used in correlating a segment of the data of a typical scatterometry mission. For this report, a one minute, eleven second section of Garden City, Kansas Mission 32 data was selected

for analysis. This section was selected because of the homogeneous nature of the terrain which allowed separation of individual scattering signatures into appropriate categories. The data appeared to be reasonably well behaved although subsequent associated scatterometry analysis showed similar data from later Garden City Missions to be invalid due to measurement recording and processing errors. Therefore, the scattering coefficients shown in this report for the various types of terrain may not be correct. However, this does not invalidate the correlation technique demonstrated herein.

II. THE CORRELATION OF SCATTEROMETRY DATA WITH AERIAL PHOTOGRAPHY

The analysis of scatterometry data begins by assemblying all records associated with the selected Mission, Flight, Line and Run. These records will consist of the following items: 1) Mission Summary Report, 2) Aerial photograph record for the selected line prepared as a mosaic, 3) Photo record of the digital control panel, and 4) Digitally processed filter plots and σ° versus Θ curves for the selected line.

The correlation procedure can be summarized as follows: First the on-off times are identified for the scatterometer and the RC-8 aerial camera operation for the selected line of data. These times are given in the several logs listed in the Mission Summary Report, The second step matches up the aerial photograph mosaic for the entire run with the scatterometer data record by converting the photo time to master control time. This process is performed by correlating record times either at the beginning or the end of the line of data. The third step selects the segment of terrain to be analyzed within the boundaries of the line and correlates σ° vs. Θ signatures to the various types of terrain. Finally, curves of average σ° vs. Θ are plotted for each category of terrain with the deviation from average indicated on the graph.

Consider first the establishment of a common time base between the photo mosaic and the digital clock. Figure 1 shows a single aerial photograph taken at camera clock time 2: 22: 21. But this time corresponds

to digital clock time 14:24:35 as shown in the accompanying photo record of the control panel. To correlate the two records, each section of the photo mosaic must be matched to the proper control panel digital clock time. This step is straightforward after the initial synchronization has been made between the two time bases. Figure 3 shows a section of the photographed record of the digital clock and the method used to indicate activation of the aerial camera. Correlation of the aerial photo record is accomplished by aligning this control panel activation time at the beginning of the line with the indicated time on the aerial photo. An example is perhaps the best way to illustrate this alignment procedure.

Table 1 indicates the relationship between the control panel time and the aerial photo clock for the selected Line and Run. It should be noted from the table that the first four control panel times illustrated in Figure 3(a) do not correspond to an aerial photo time. This is because two adjacent control panel times that differ by one second or less at the beginning of a run indicate the scatterometer recorder is receiving a starting mark, or that the aerial cameras are being activated, or that both occur at the same time as shown in Figure 3(b). The fifth control panel in Figure 3(a) gives the control panel time for the first aerial photo. Because the processed scatterometry data uses the control panel digital time for its time base, the aerial photo record is now properly time marked for relating it to the scatterometer data. Figure 4 illustrates a segment of flight line aerial photographs that have been properly time marked for correlation purposes using Table 1.

The second step involves identifying the scatterometry time data relative to the control panel time. These data are processed with a time scale identical to the control panel time. Therefore, this step simply

selects the data appropriate to the selected aerial photo record at the desired viewing angle. Figure 5 shows the correspondence of the control panel time during scatterometer 'start' time and the related processed data record for an angle 2.5° aft of the nadir. Scatterometry data for this correlation may be used in two formats. Figure 6(a) and 6(b) illustrate a σ° (differential scattering cross section) versus Θ (incident angle) curve for two resolution cells. Figure 6(c) is a relative voltage versus time curve for a specific radar incident angle. The former curves are determined from the same information used to generate the latter curves by computer techniques; therefore, either or both formats may be used in the correlation process. For this report, σ° versus Θ curves were used together with a computer printout of σ° versus resolution cell. Table 2(a) lists the resolution cells in numerical order as they occur along a segment of Run 1 together with the values of σ° versus Θ. From this table a curve of σ° versus resolution cell for any angle can be plotted as illustrated in Figure 7.

The next step in the correlation procedure involves the alignment of the plotted scatterometry data with the photo mosaic. This can be accomplished by measuring the average time per unit length for the mosaic over the entire flight line and using this value for all σ° versus time plots. Because there are σ° versus time curves for each of several angles, this alignment can be accomplished for any angle. However, to show the correspondence of electronic data with major terrain characteristics, the incidence angle has been selected which best demonstrates the interrelationship. Figure 8 shows the alignment of scatterometry data taken 2.5° aft of the nadir. These data were more closely related to the photo mosaic than those for other angles, probably due to the radar swath at this angle falling within the boundaries of the homogeneous fields despite any aircraft crabbing or changes in attitude.

The next step in the analysis defines the physical boundaries that enclose homogeneous surfaces on the photo mosaic. For most cases appropriate studies of the terrain will serve to identify these homogeneous areas. This was relatively easy for Run 1 since the boundaries were rectangular in nature indicated by the shaded regions in Figure 9. Because the scattering

characteristics differ for each of these homogeneous areas, it follows that the time history curves should have boundaries separating returns from adjacent areas of different content. Thus, the final alignment consists of slightly varying the terrain boundaries with the time history boundaries by expanding and contracting the time history curve grid within reasonable limits. Reasonable limits are justified by assuming certain aircraft orientations, or by noting the error introduced by a control panel clock indicating seconds while σ° versus time curves are plotted in one-hundredths of a second, or by noting variations in aircraft velocity.

Table 3 indicates the classification of each resolution cell by means of Figure 9 and information on each field supplied by agricultural geographers. (Note that NASA/MSC numbers fore and aft resolution cells differently as shown in Table 3 and in Figures 6(a) and 6(b).) In this case resolution cell "649 aft" was approximately resolution cell "615 fore" because the former has nadir time T_N that was 14: 24 34.46 as marked on Figure 6(a) and the latter has a T_N that was 14:24 34.36 as marked on Figure 6(b). The result of the correlation performed for any incident angle allows an extrapolation of the correlation to any of the several angles, fore and aft, using the same grid arrangement. Examples of this are shown for the family of aft curves in Figures 10(a) to 10(g).

An alternate method of plotting scatterometer data uses the computer data printout shown in the upper corner of Figure 11. Note that these data are relative voltage levels plotted on semi-log paper. This is equivalent to the linear db scale of Figures 10. Because the time scale (abscissa) of the computer plotted data differs from the photo mosaic, the plot must be rescaled as indicated in Figure 11. The time scaling factors for use with the computer plots are derived in the Appendix. For purposes of this analysis, however, it was easier to simply use the tabular printout of σ° versus resolution cell for the construction and correlation of Figures 10.

A catalog of scatterometer data may now be compiled for the sample run by replotting the data shown in Figures 10(a) through 10(g) as σ° versus Θ data shown in Figure 12. Deviations from average signature response are plotted in Figure 13. These figures represent the desired result of the

preliminary analysis of scatterometer data since the data signatures have been correlated with the nature of the ground terrain. Figures 12 demonstrate that similar types of terrain do indeed have similar scatterometry signatures. Figures 13(c) and 13(d) are plots of average σ^{o} versus Θ for four categories of the measured terrain. The upper and lower limits of variation of σ^{o} are indicated on the curves. The returns for the several categories are reasonably consistent for the number of samples of terrain type used in the averaging process.

III. CONCLUSIONS

An analysis has been presented which shows the technique that must be used to correlate radar scatterometry data with the nature of ground terrain. Perhaps the most significant problem in performing this correlation is the lack of a time-synchronized data gathering and processing system. In the future, scatterometry missions should be designed such that all sensors on board the aircraft have the same time scale. Data processing should be accomplished with the printed output compatible with the time scale of the photo mosaic. In this way, data correlation could be performed instantaneously without the necessity of tabulating and replotting vast amounts of data.

APPENDIX

Time Relationships for Scatterometry Data

The instantaneous data record of the scatterometer represents simultaneous measurements from all resolution cells within the antenna pattern. In order that the measured data at each angle represent the appropriate resolution cell, it is necessary to correct the time scales of the data at each doppler filter output. This correction factor ΔT can easily be derived from the position and velocity records of the aircraft.

Consider Figure 14 which shows the relevant geometry. For a particular incident angle Θ not equal to zero, the actual radar return from a given resolution cell occurs at time T_Θ. In order to plot σ° versus Θ curves for a particular ground cell, all measurement times are referenced to T_N defined at $\Theta = 0$. Thus, the correction factor ΔT for each angle Θ is

$$\Delta T = T_N - T_\Theta$$

where from the geometry of Figure 14:

$$T_N - T_\Theta = \frac{h \tan \Theta}{v}$$

Where: T_N = measurement time for $\Theta = 0$
T_Θ = measurement time at angle Θ
h = aircraft altitude
Θ = incidence angle
v = aircraft velocity.

As an example, for Mission 32 with

$\Theta = 45°$ aft $= -45°$

$h = 3000$ ft.

$v = 240$ ft/sec.

$\tan \Theta = \tan (-45°) = -1$

$$\Delta T = T_N - T_\Theta = - \frac{3000 \text{ ft}}{240 \text{ft/sec}} = -12.5 \text{ sec.}$$

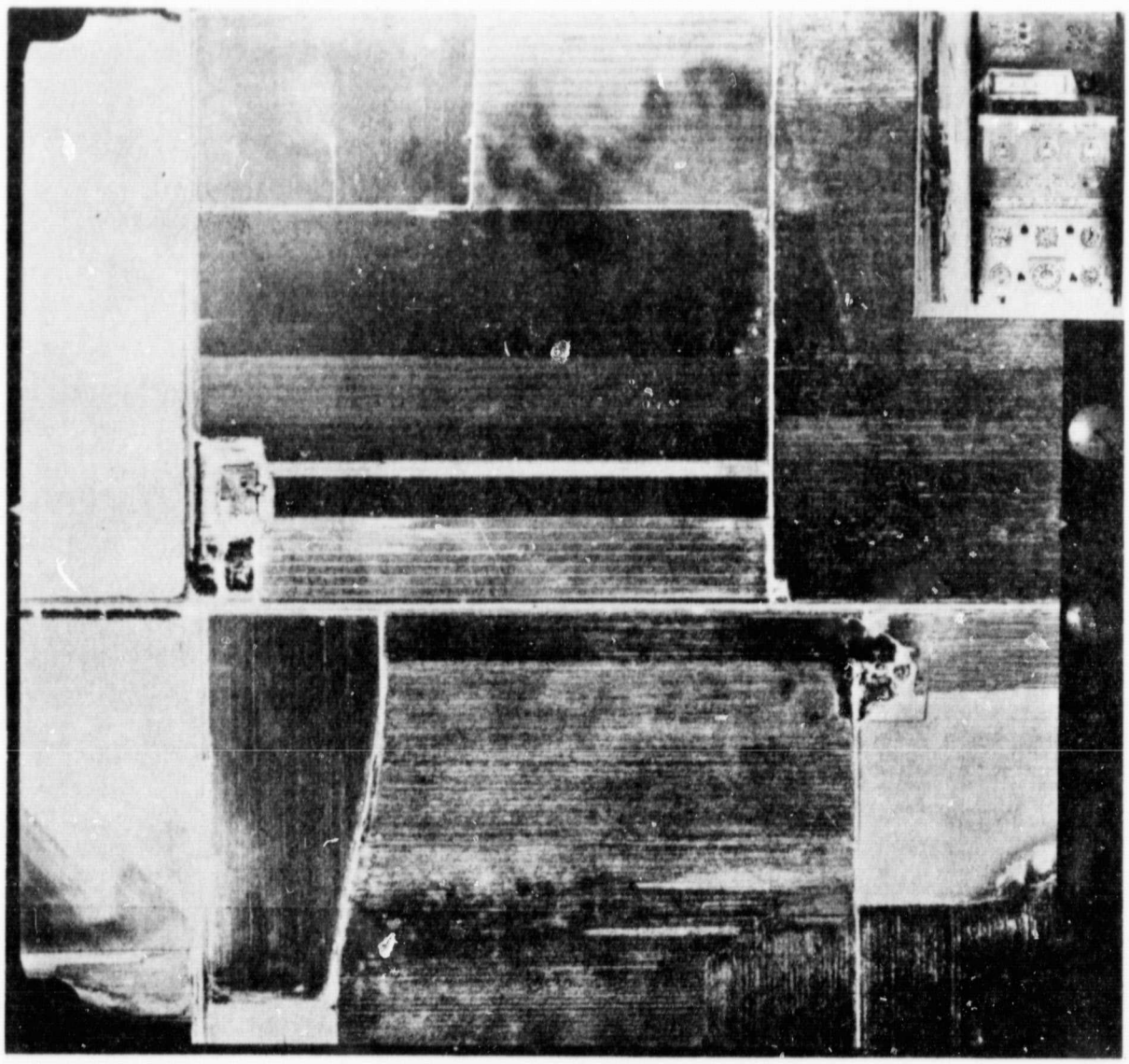

Figure 1. Aerial Photo and Corresponding Control Panel Photo from Flight 1, Line 1, Run 1, Mission 32, Site 76 (Garden City, Kansas), 9-19-1966

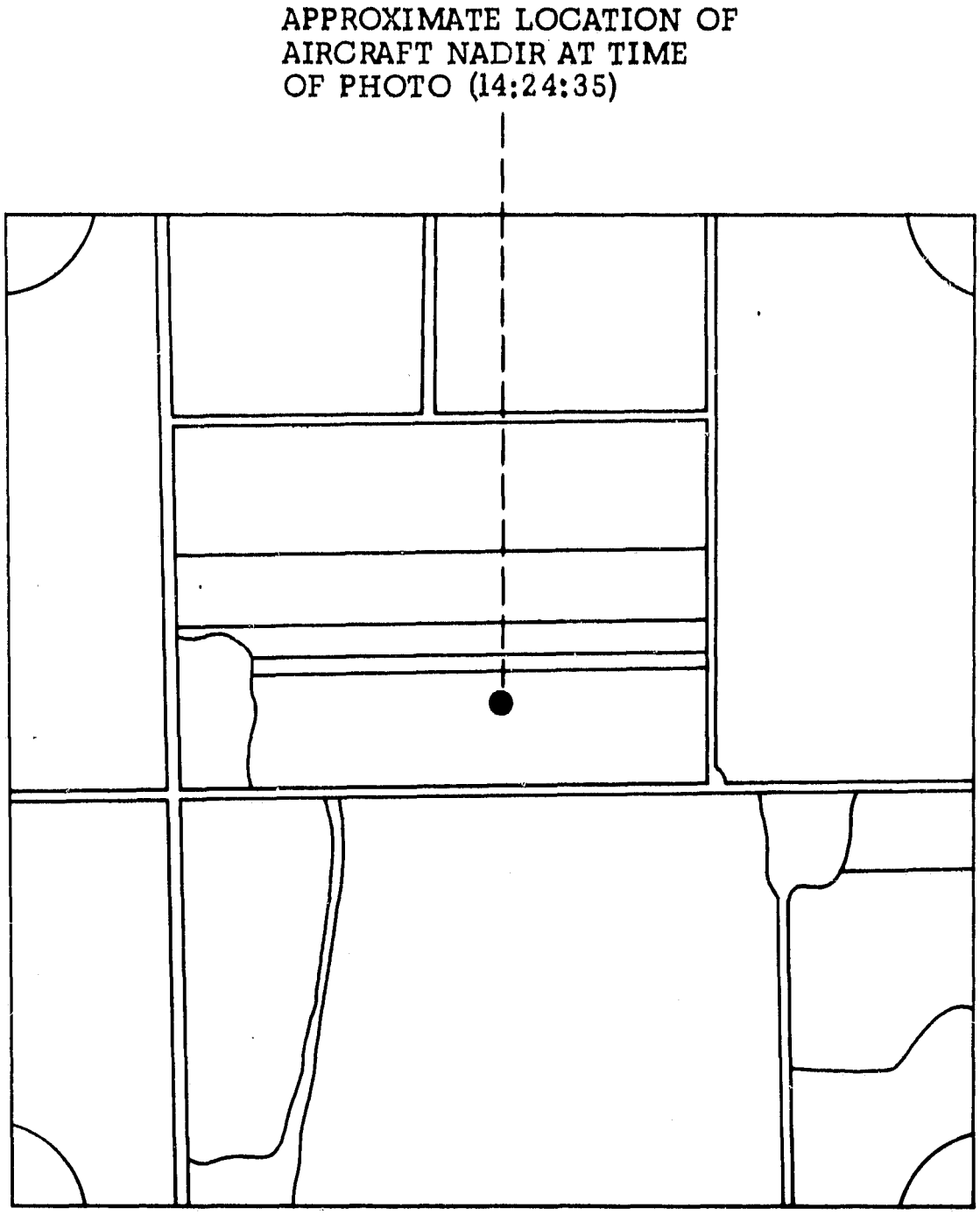

Figure 2. SKETCH OF THE AERIAL PHOTO SHOWN IN FIGURE 1 AND THE APPROXIMATE LOCATION OF THE AIRCRAFT NADIR AT THE TIME THE PHOTO WAS TAKEN

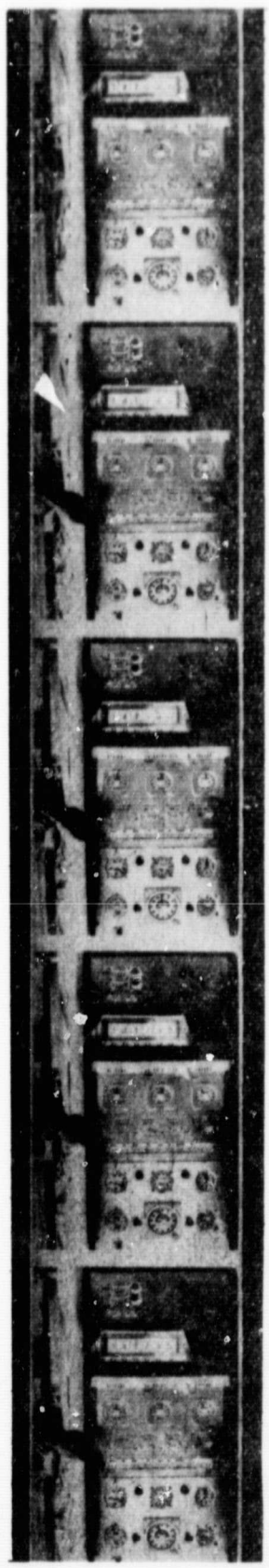

Time of Initial Photo for Run 1 (14:19 46)

Time that Aerial Cameras are Activated (14:19 40)

Time Indicating that Scatterometry Recorder has been Given a Start Mark that Data Processors can Identify and Use to Assign Control Panel Time to all Processed Data.

Figure 3(a) Control Panel Film Giving Scatterometry Data Recorder Start Mark Time, Aerial Camera Start Time, and the Time of the First Aerial Photo.

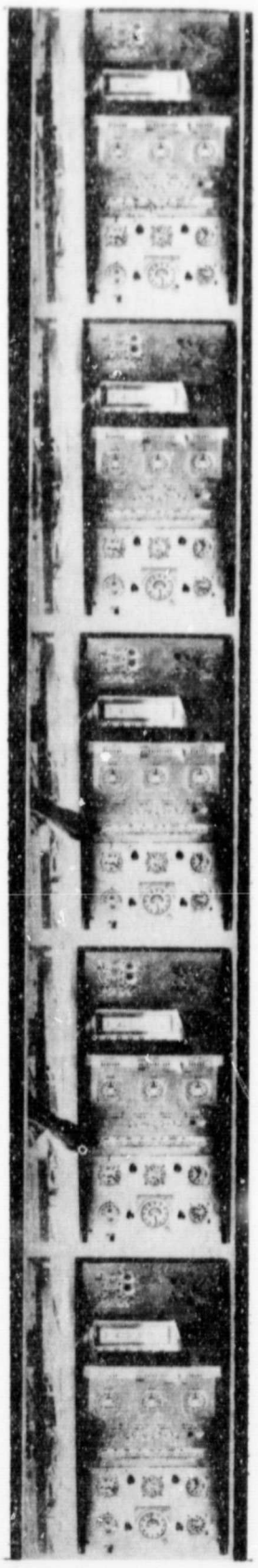

Time of Second Aerial Photo for Run 4
(14:30 11)

Time of First Aerial Photo for Run 4
(14:30 04)

Indicates that Scatterometry Data Recorder
Given Start Mark and Aerial Camera
Activated at Time (14:30 00)

Time of Last Aerial Photo for Run 1
(14:25 29)

Figure 3(b) Aerial Camera is Activated and Scatterometry Recorder is Given a Start Mark at the Identical Time.

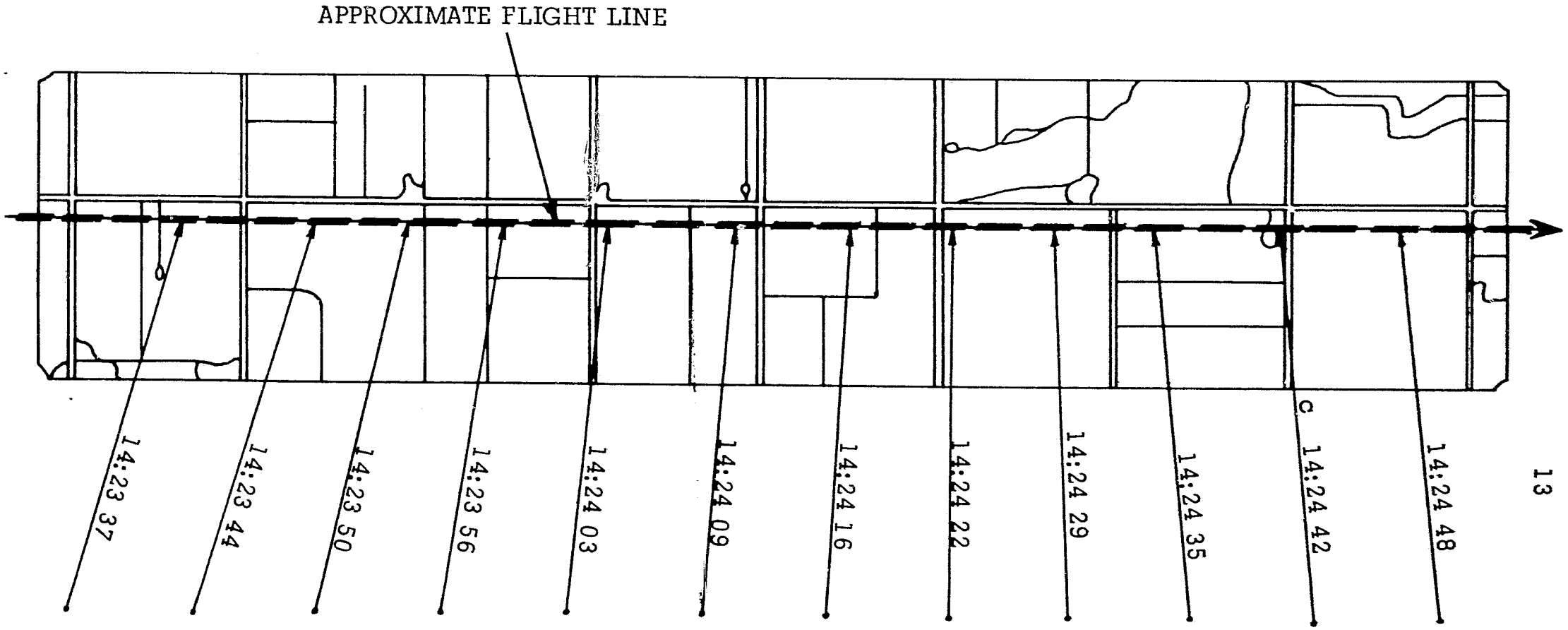

Figure 4. PHOTO MOSAIC FORMED FROM INDIVIDUAL AERIAL PHOTOS AND THE APPROXIMATE LOCATION OF THE AIRCRAFT NADIR AT VARIOUS CONTROL PANEL TIMES.

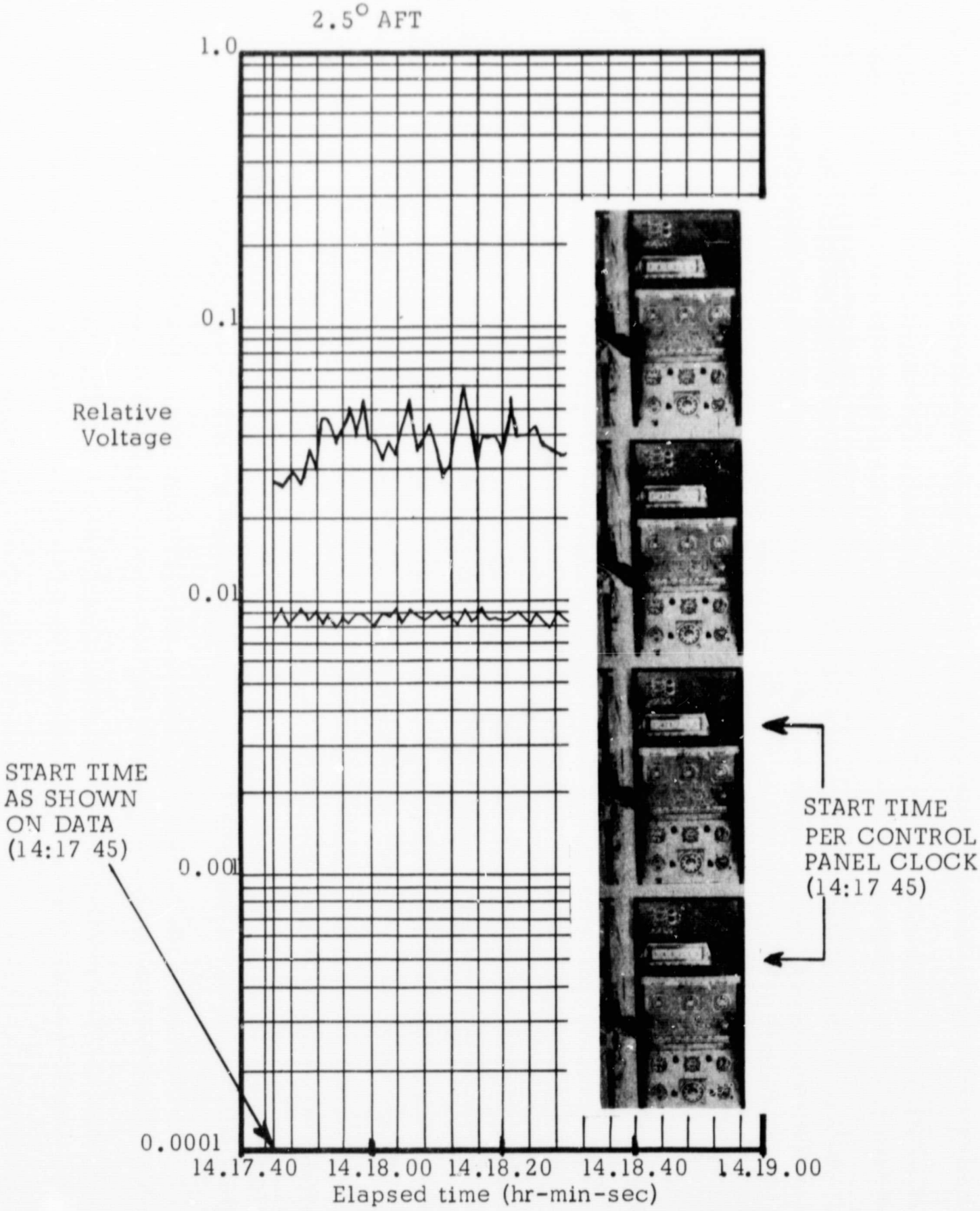

Figure 5. CORRESPONDENCE OF CONTROL PANEL TIME WITH PROCESSED DATA TIME.

MSC-6299-

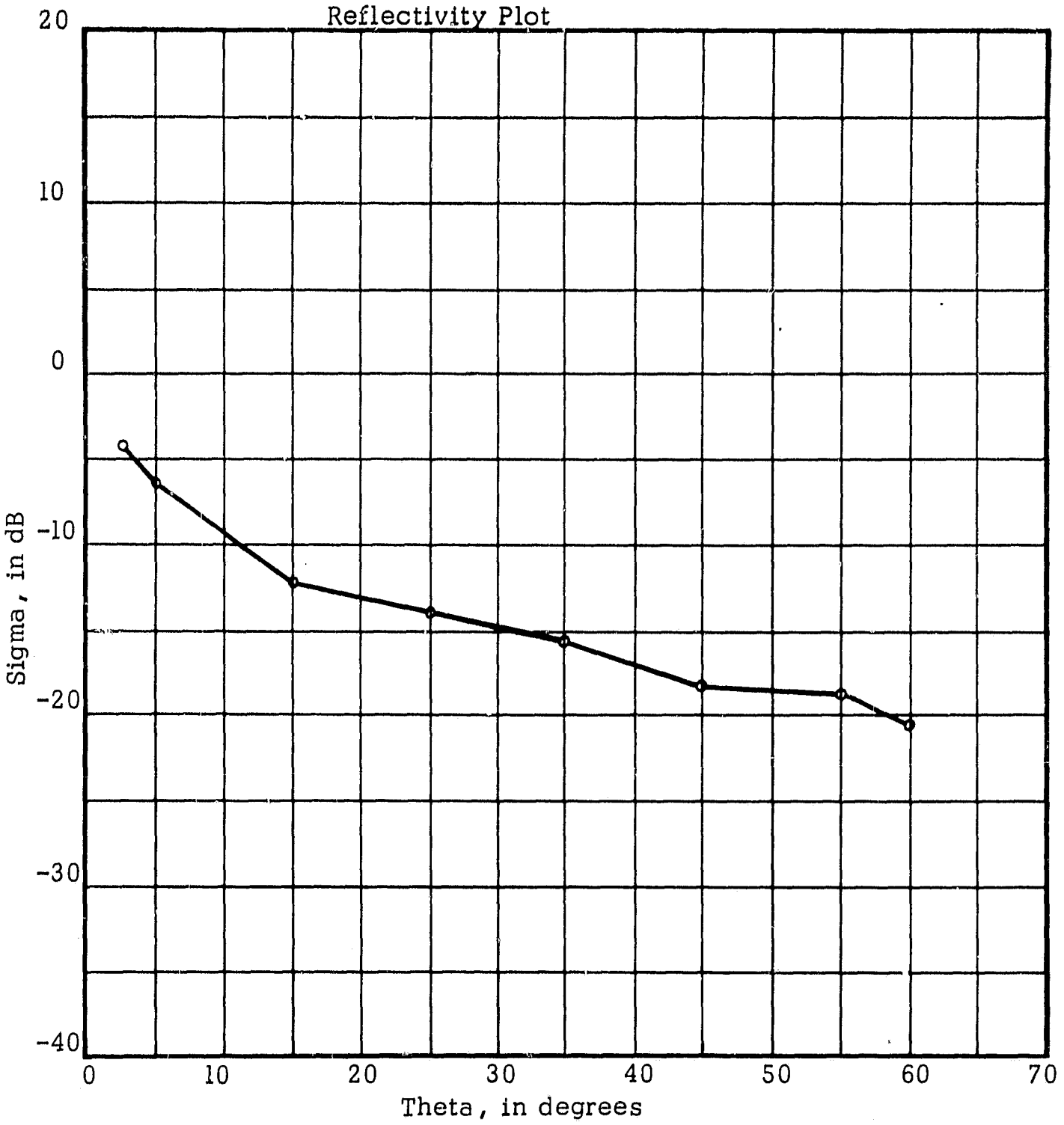

Figure 6(a). AVERAGE RETURN (σ°) FROM A PARTICULAR RESOLUTION CELL (649 AFT) VERSUS VARIOUS AFT ANGLES (Θ). NADIR TIME T_N = 14:24 34.46.

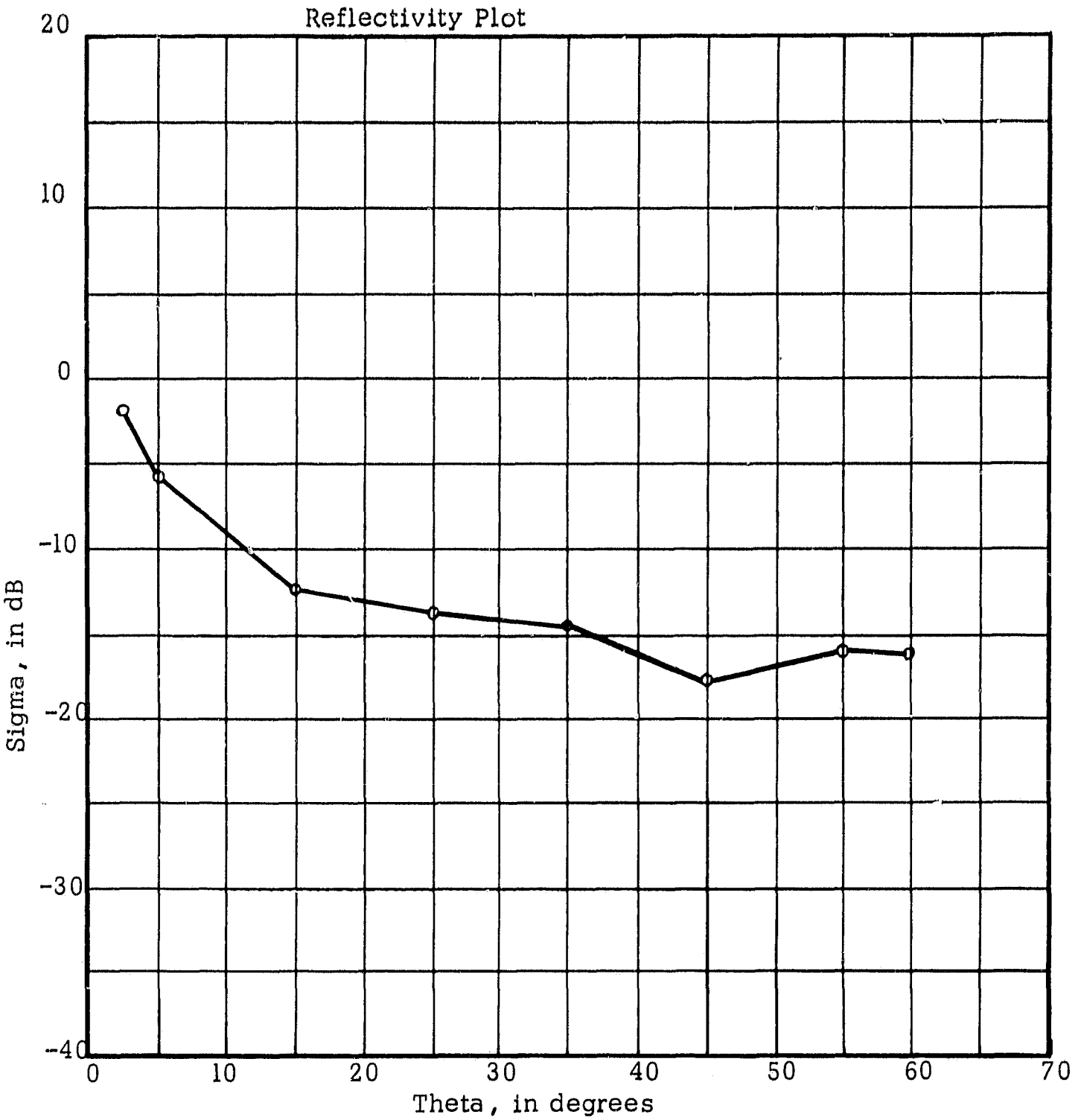

Figure 6(b). AVERAGE RETURN (σ°) FROM A PARTICULAR RESOLUTION CELL (615 FORE) VERSUS VARIOUS FORE ANGLES (Θ) NADIR TIME T_N = 14:24 34.36

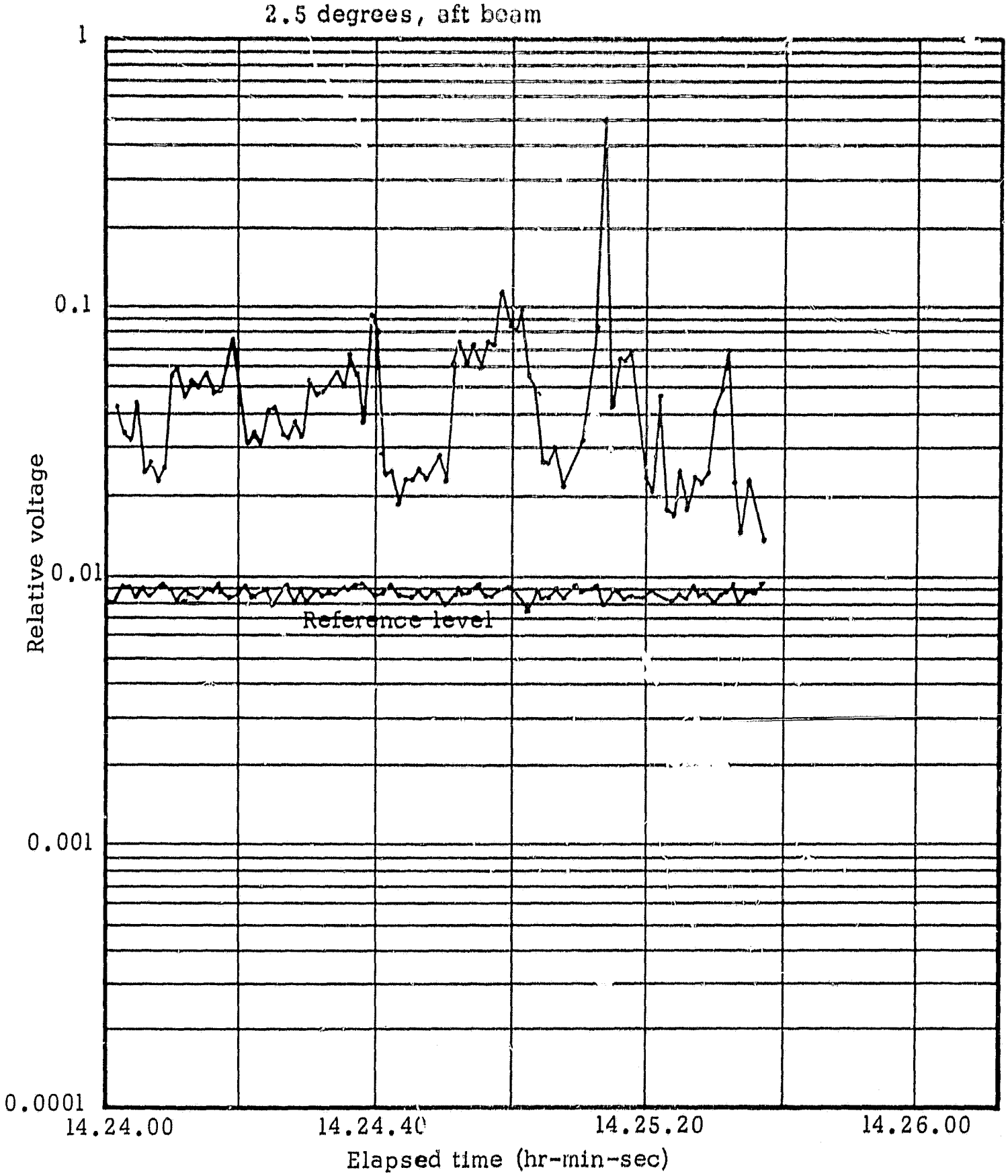

Figure 6(c). COMPUTER PLOTTED SCATTEROMETRY RETURN SIGNAL VERSUS TIME FOR A SEGMENT OF FLIGHT1, LINE 1, RUN 1, MISSION 32, SITE 76 (GARDEN CITY, KANSAS), 9-19-1966, 2.5° AFT.

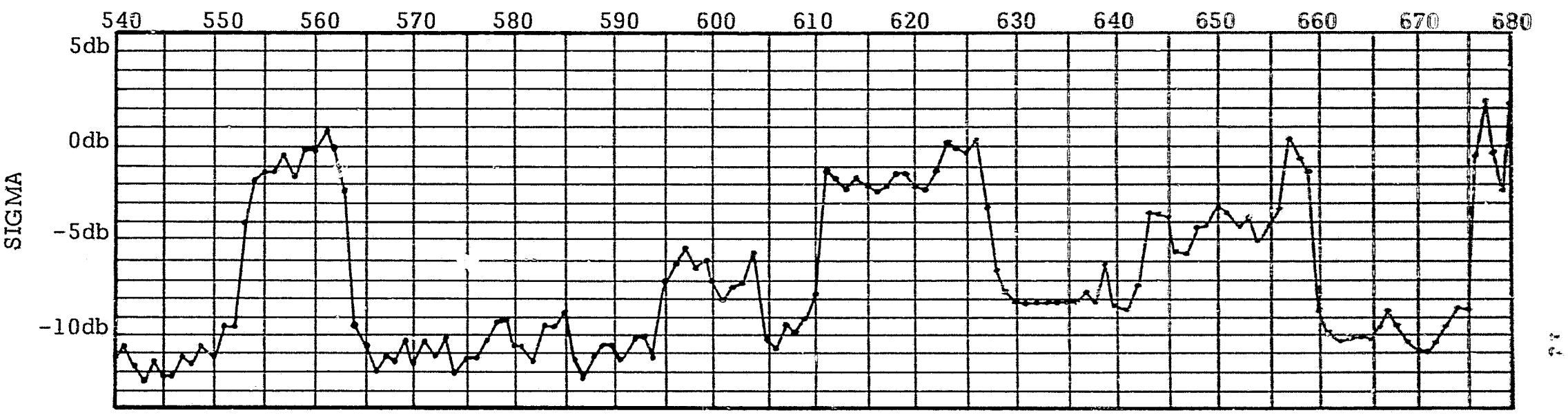

Figure 7. PLOT OF σ° VERSUS RESOLUTION CELL FOR INCIDENCE ANGLE OF 2.5° AFT, DERIVED FROM σ° vs Θ DATA.

RESOLUTION CELL NUMBER

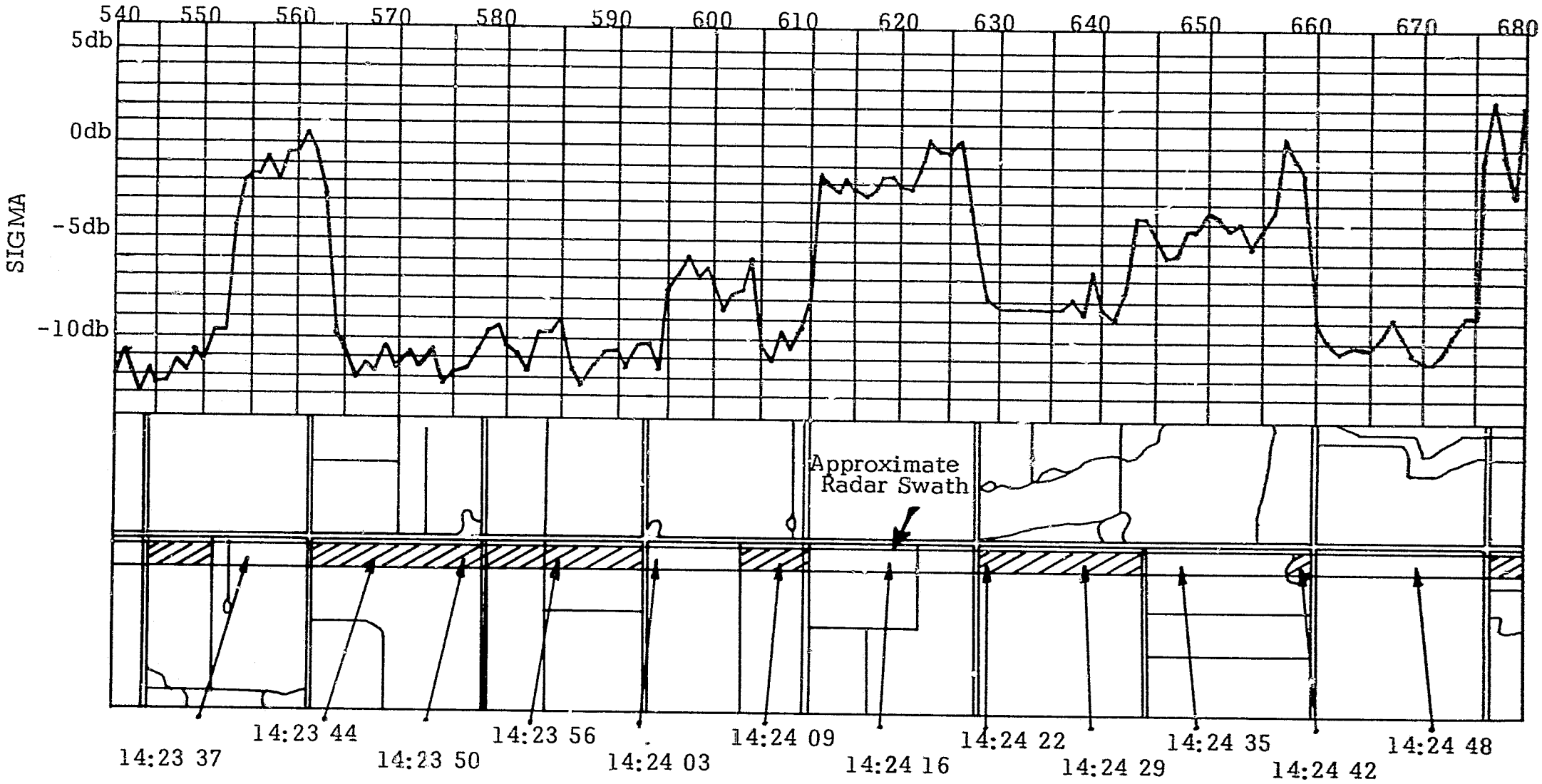

Figure 8. INITIAL ALIGNMENT OF SCATTEROMETRY DATA AND PHOTO MOSAIC FOR 2.5° AFT.

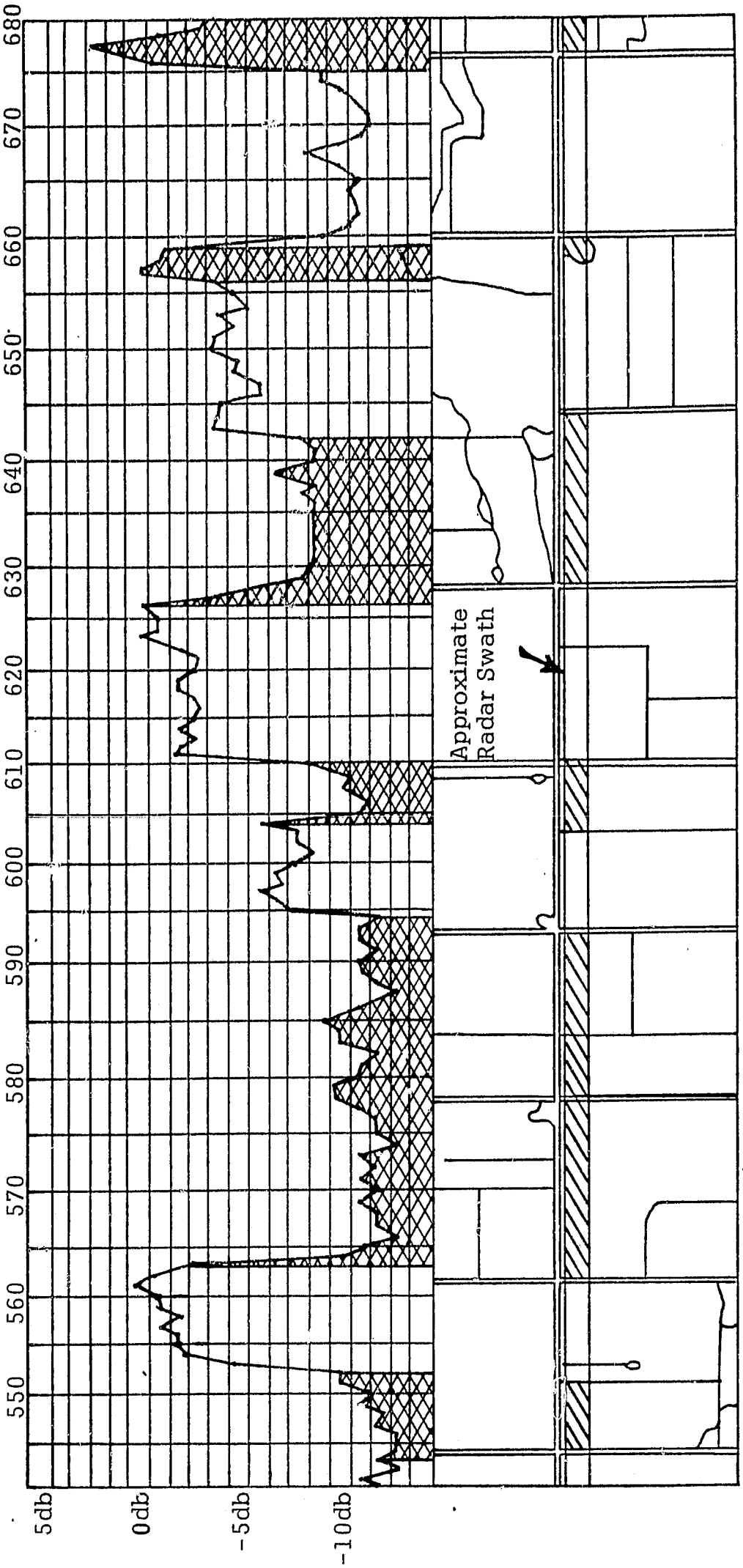

Figure 9. FINAL ALIGNMENT OF SCATTEROMETRY DATA VERSUS PHOTO MOSAIC FOR AN ANGLE OF 2.5° AFT.

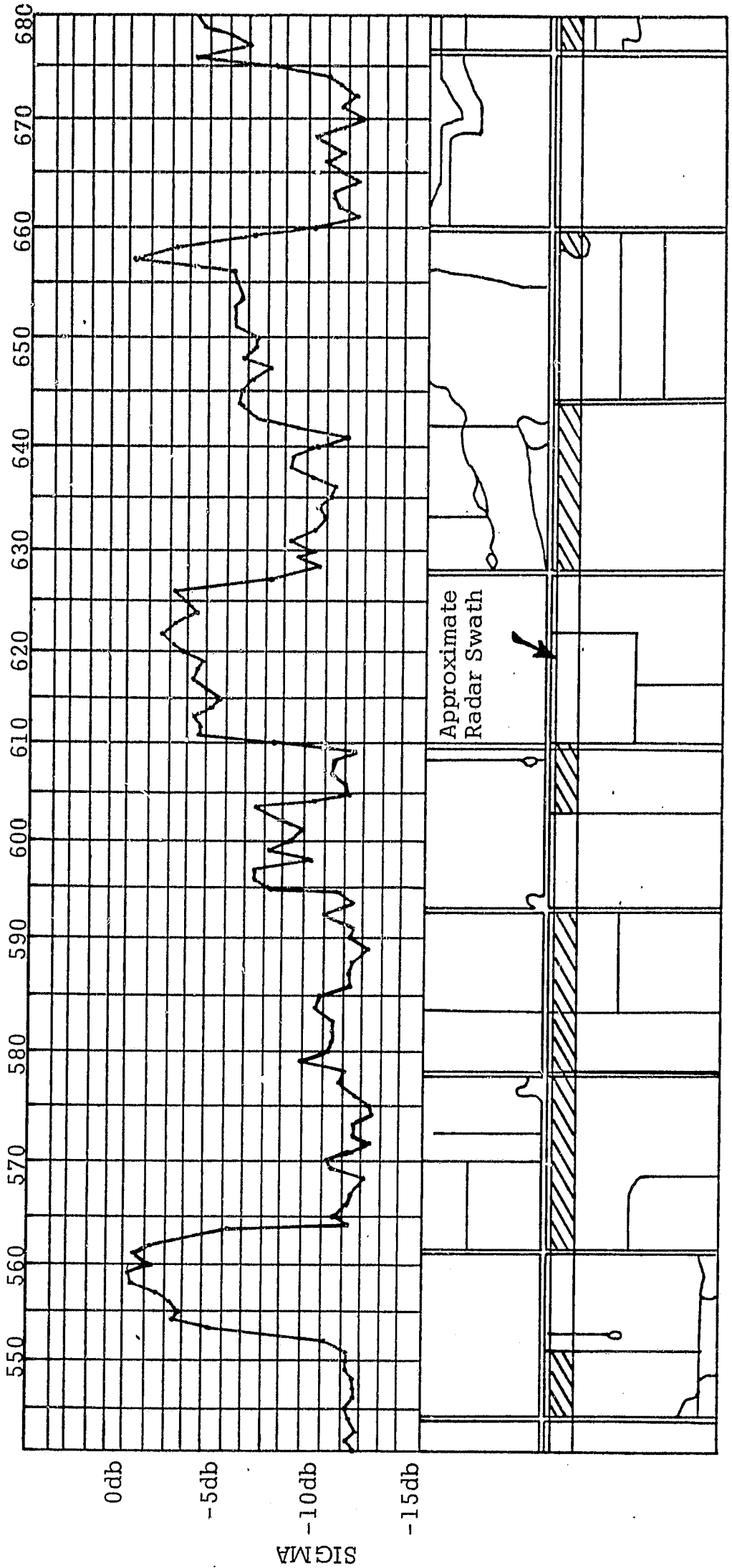

Figure 10(a). THE CORRELATION OF SCATTEROMETRY DATA AND PHOTO MOSAIC FOR AN ANGLE OF 5° AFT.

RESOLUTION CELL NUMBER

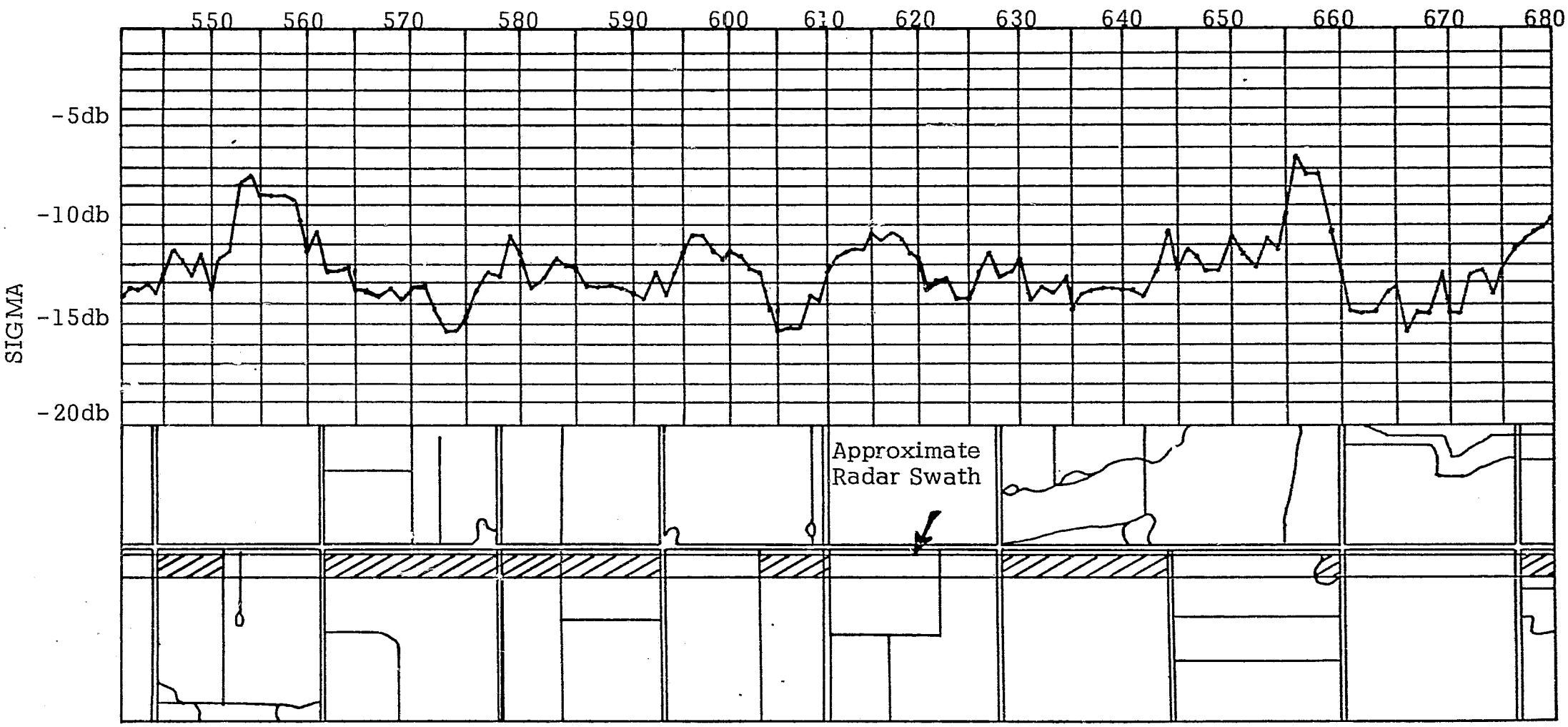

Figure 10(b). THE CORRELATION OF SCATTEROMETRY DATA AND PHOTO MOSAIC FOR AN ANGLE OF 15° AFT.

RESOLUTION CELL NUMBER

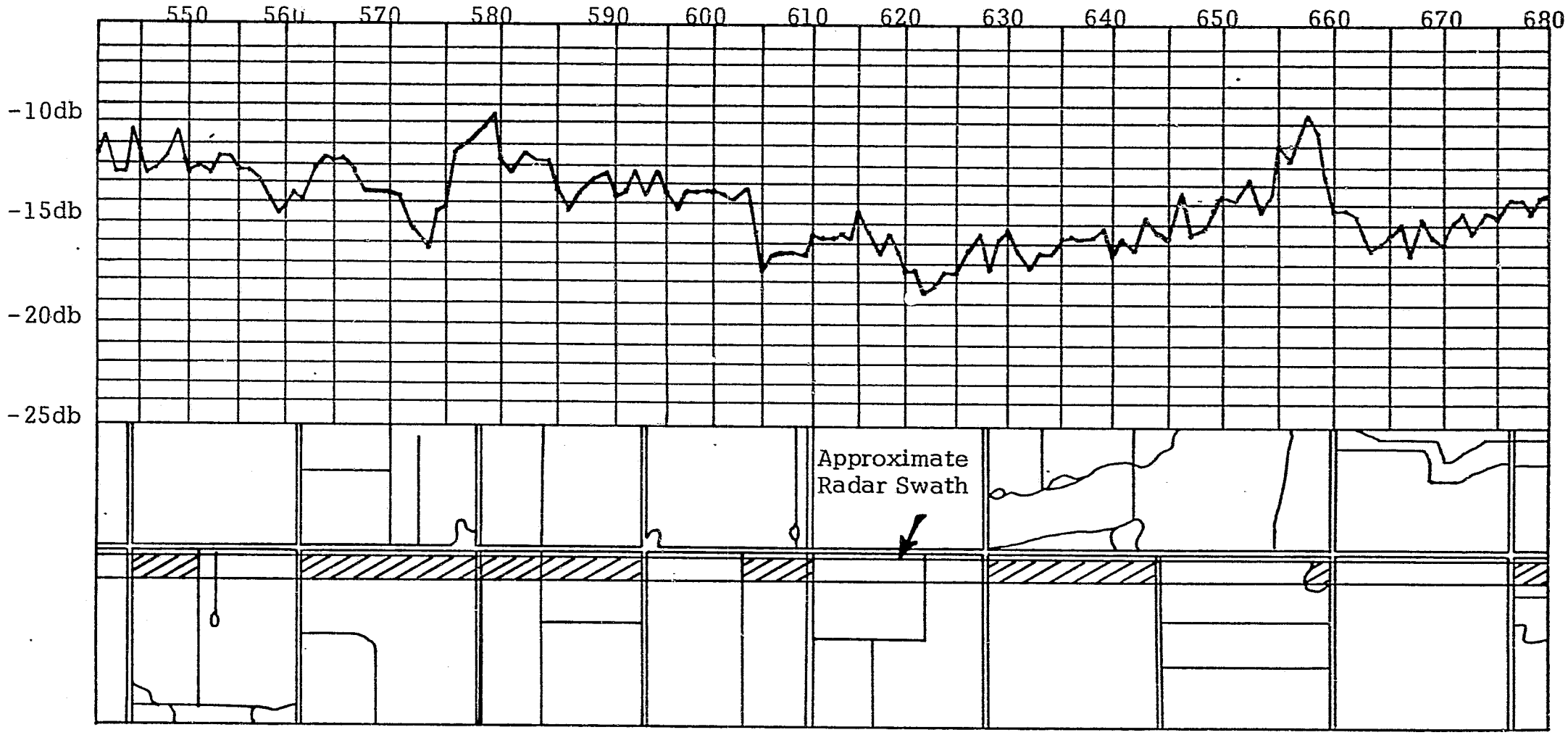

Figure 10(c). THE CORRELATION OF SCATTEROMETRY DATA AND PHOTO MOSAIC FOR AN ANGLE OF 25° AFT.

RESOLUTION CELL NUMBER

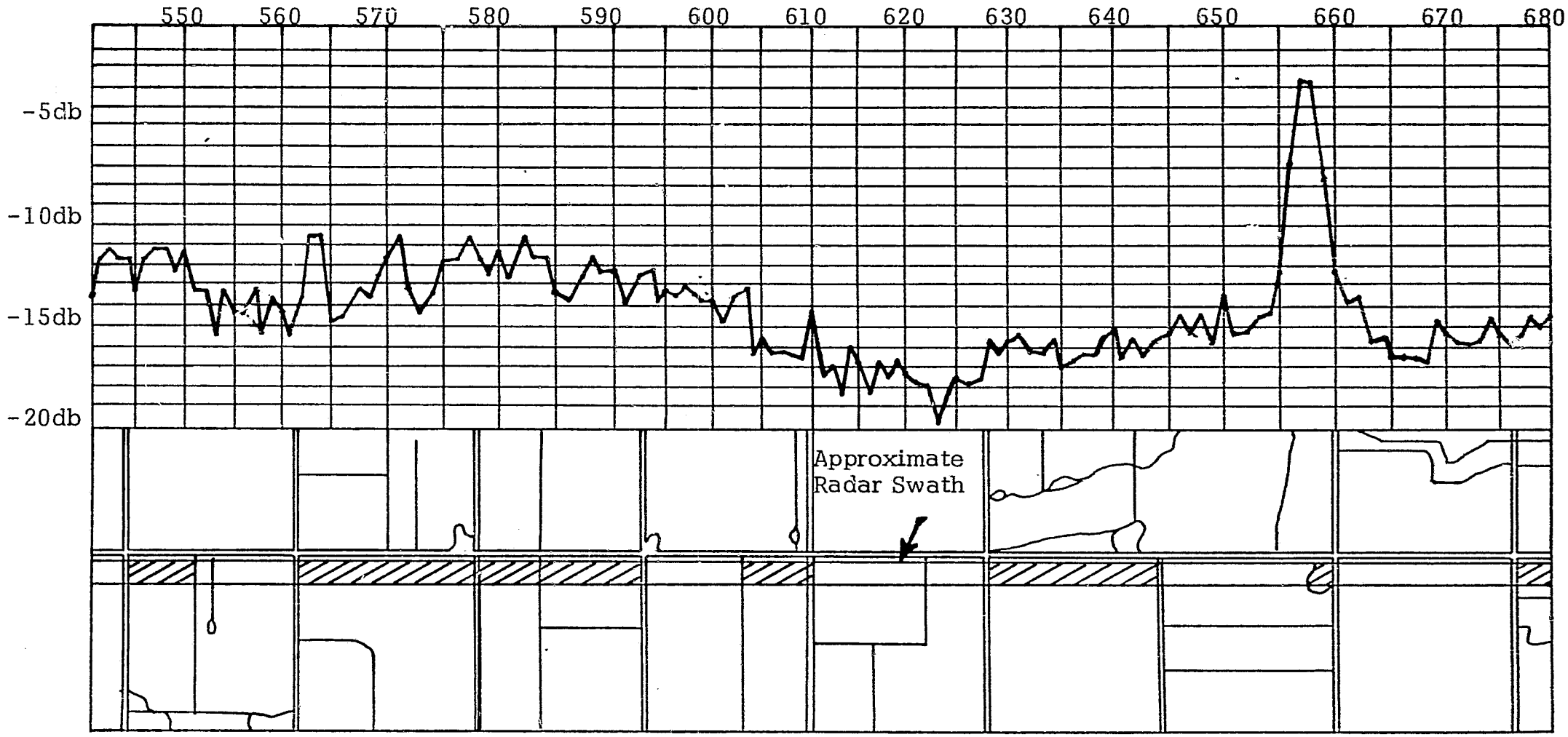

Figure 10(d). THE CORRELATION OF SCATTEROMETRY DATA AND PHOTO MOSAIC FOR AN ANGLE OF 35° AFT

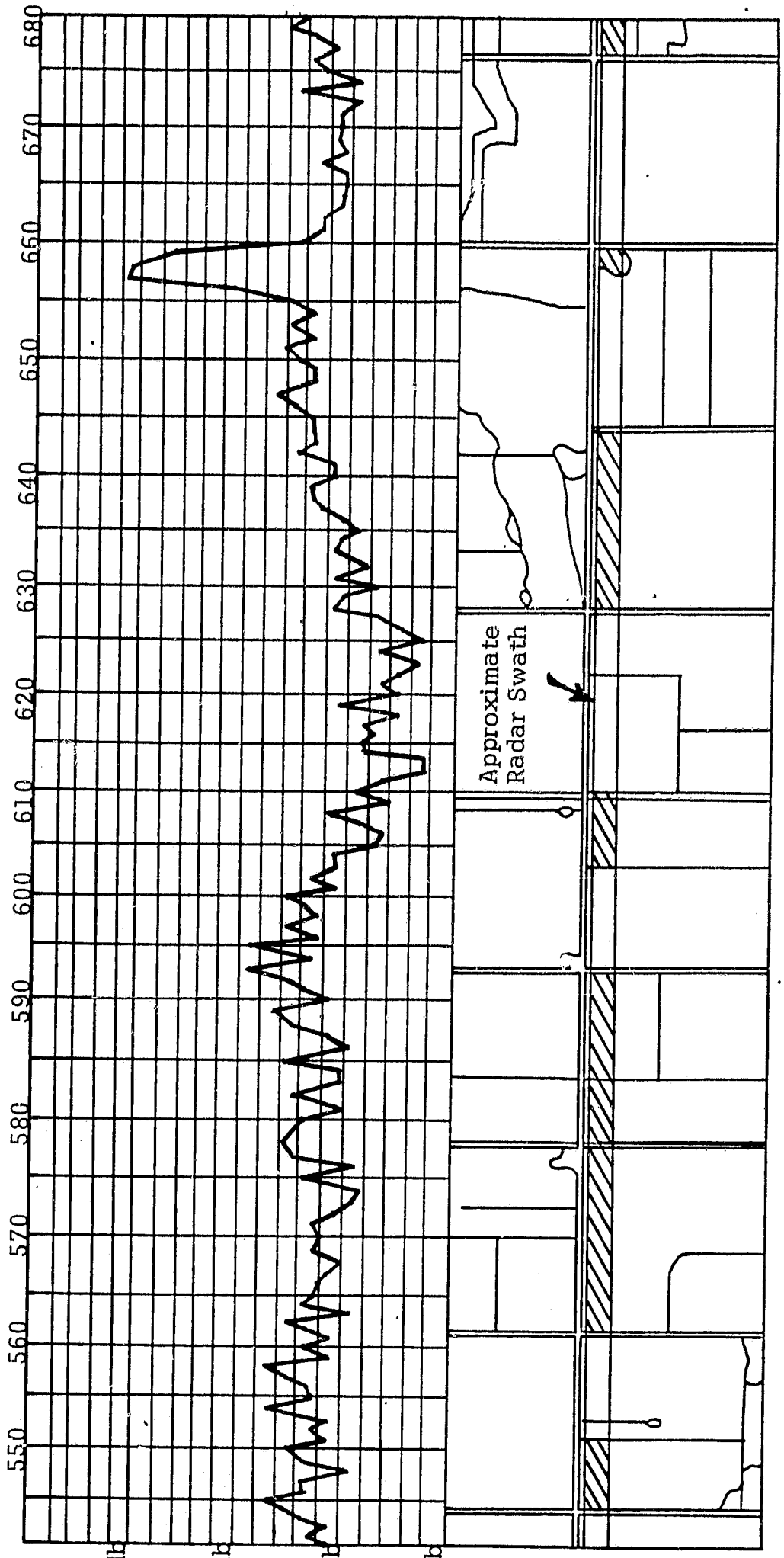

Figure 10(e). THE CORRELATION OF SCATTEROMETRY DATA AND PHOTO MOSAIC FOR AN ANGLE OF 45° AFT.

RESOLUTION CELL NUMBER

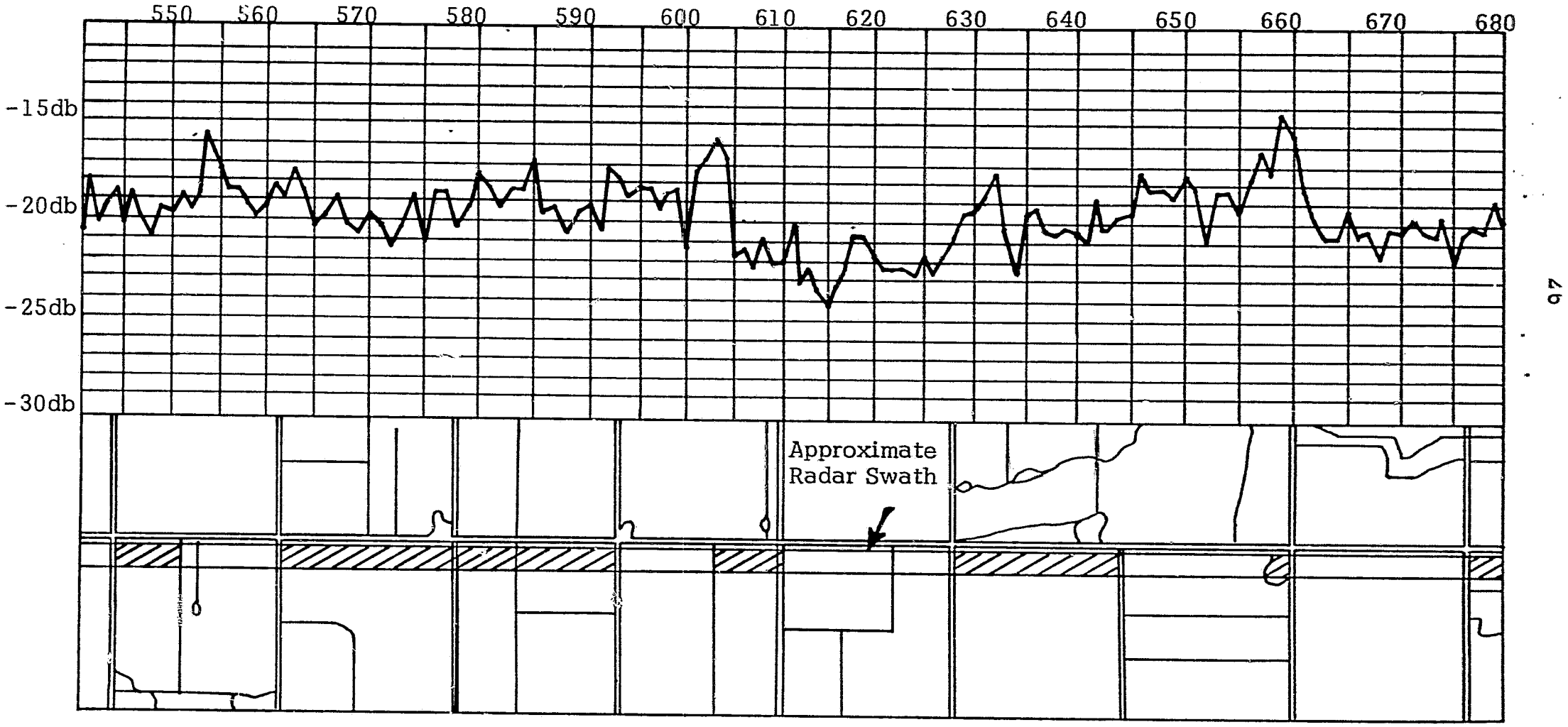

Figure 10(f). THE CORRELATION OF SCATTEROMETRY DATA AND PHOTO MOSAIC FOR AN ANGLE OF 55° AFT.

RESOLUTION CELL NUMBER

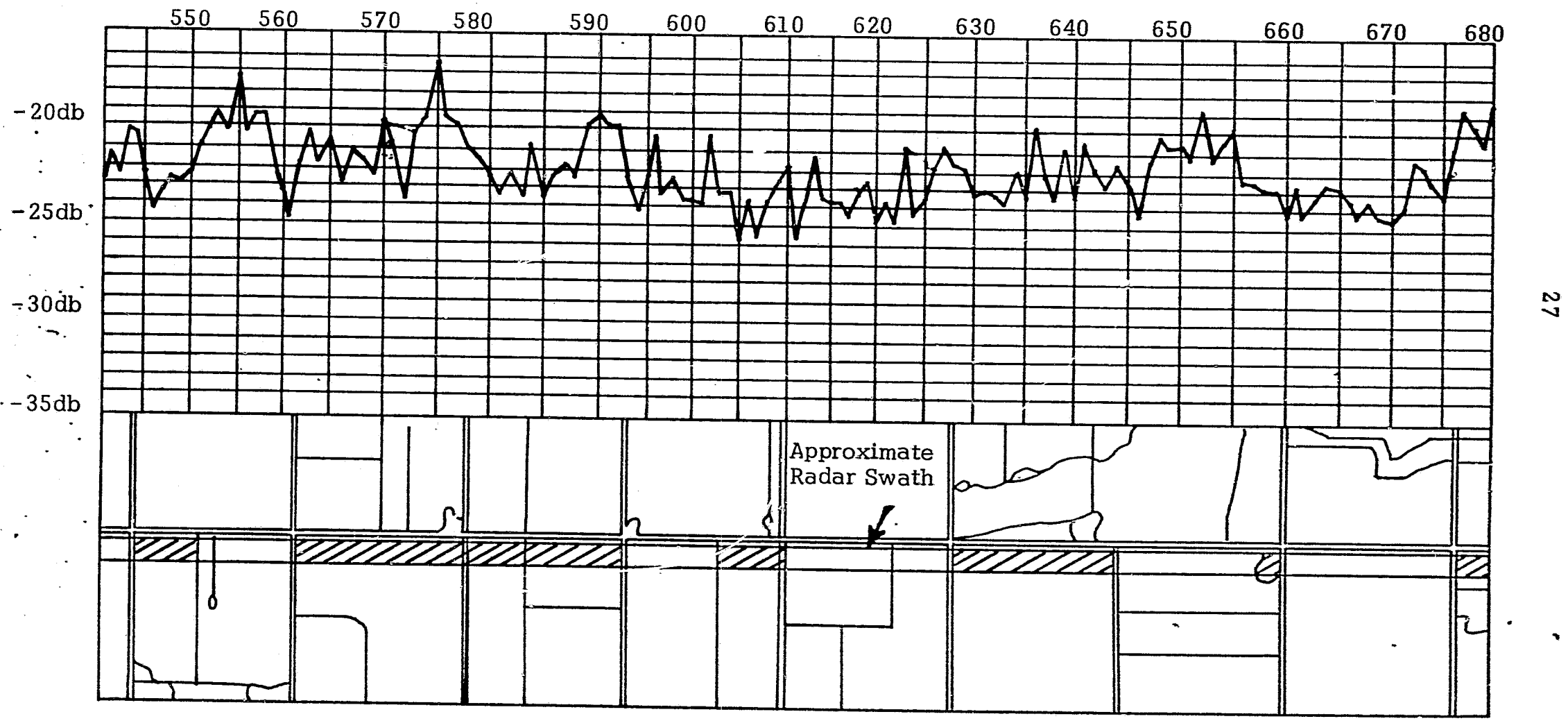

Figure 10(g). THE CORRELATION OF SCATTEROMETRY DATA AND PHOTO MOSAIC FOR AN ANGLE OF 60° AFT.

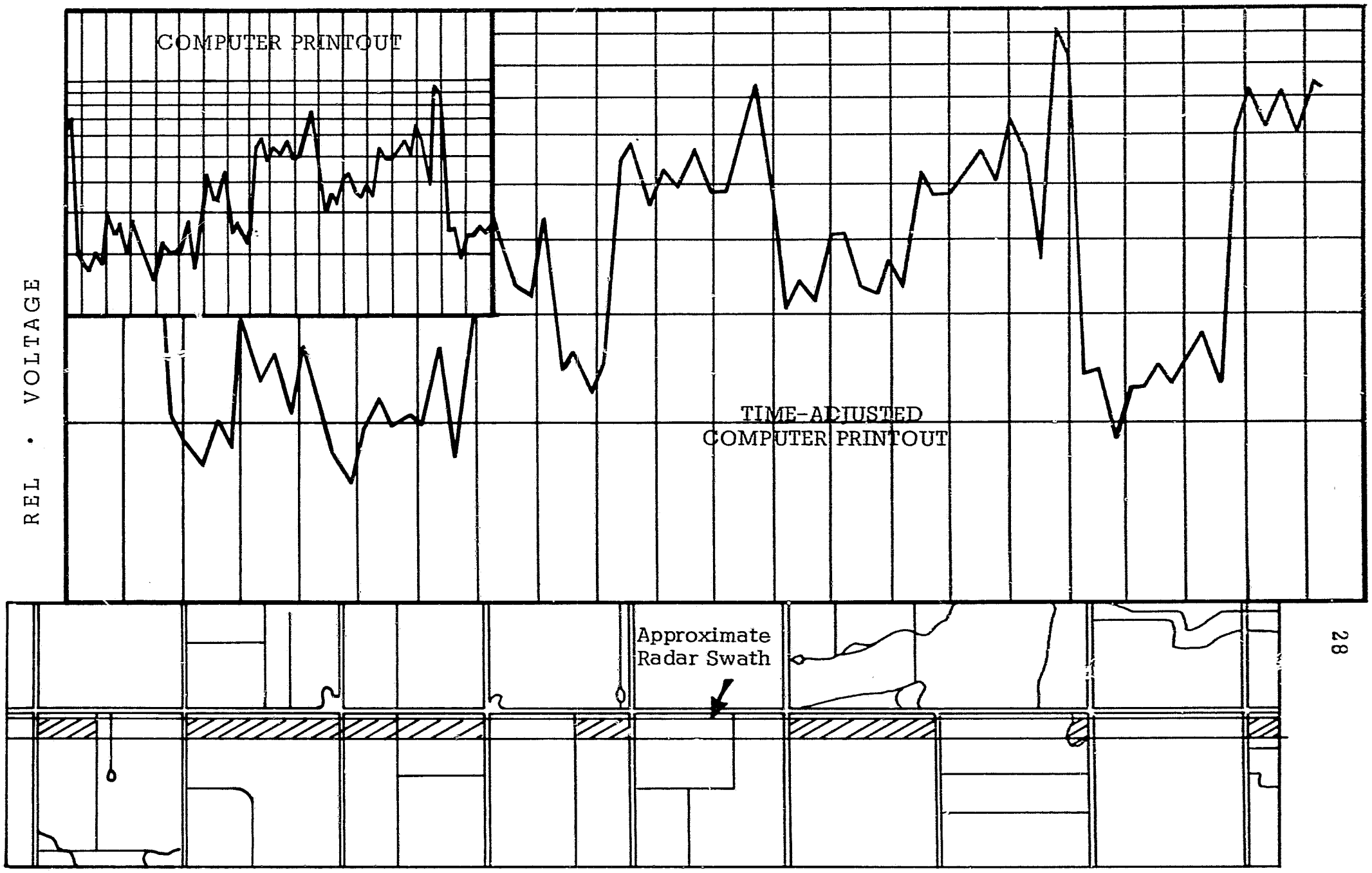

Figure 11. CORRELATION OF COMPUTER PLOTTED SCATTEROMETRY DATA WITH PHOTO MOSAIC FOR AN ANGLE OF 2.5° AFT.

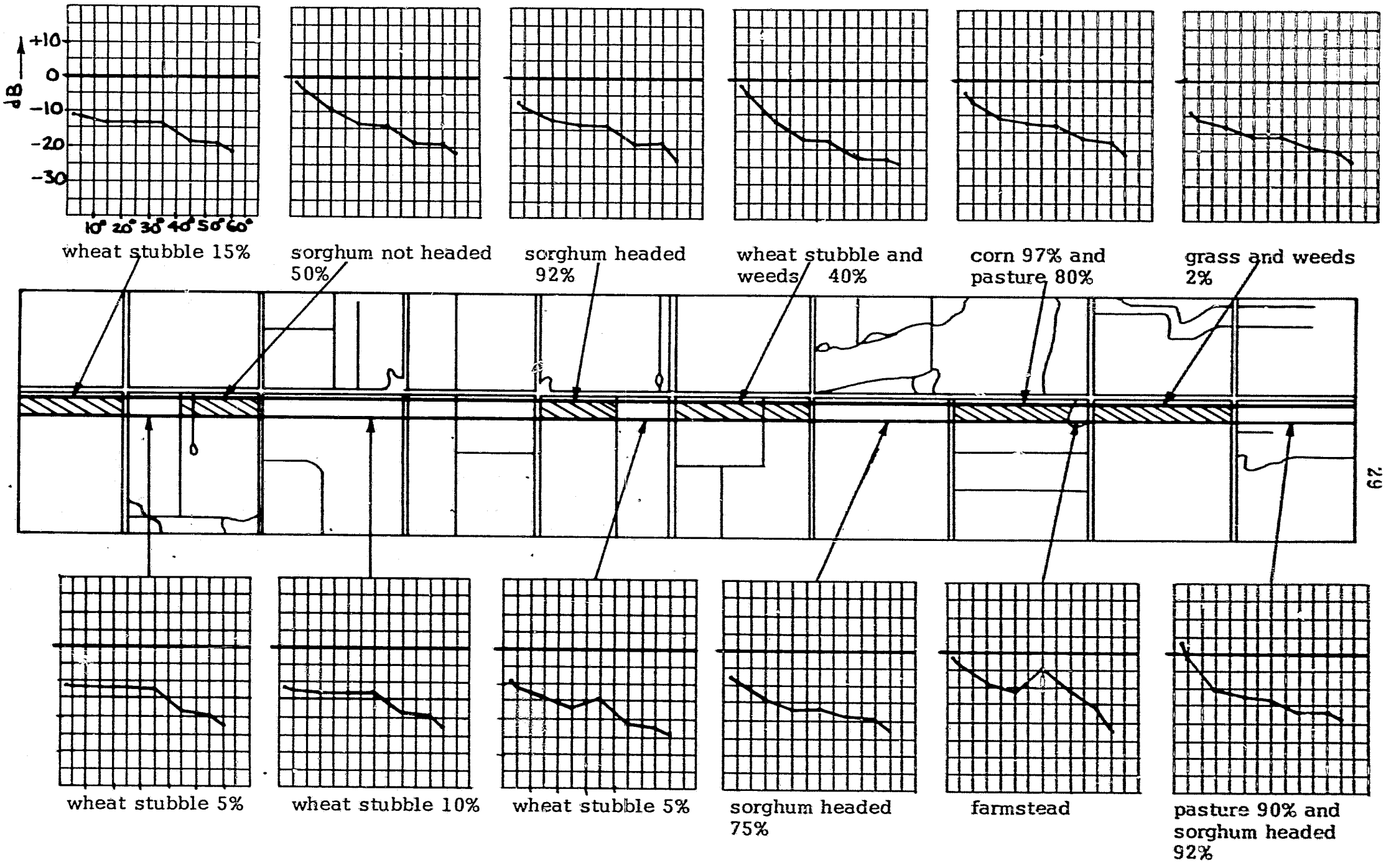

Figure 12(a). AVERAGE SCATTEROMETRY σ° (IN DB) FOR EACH CONTINUOUS AND HOMOGENEOUS FIELD VERSUS AFT INCIDENCE ANGLE Θ FOR FLIGHT 1, LINE 1, MISSION 32, SITE 76 (GARDEN CITY, KANSAS), MILES' 9, 10, 11, 12, AND 13, 9-19-1966.

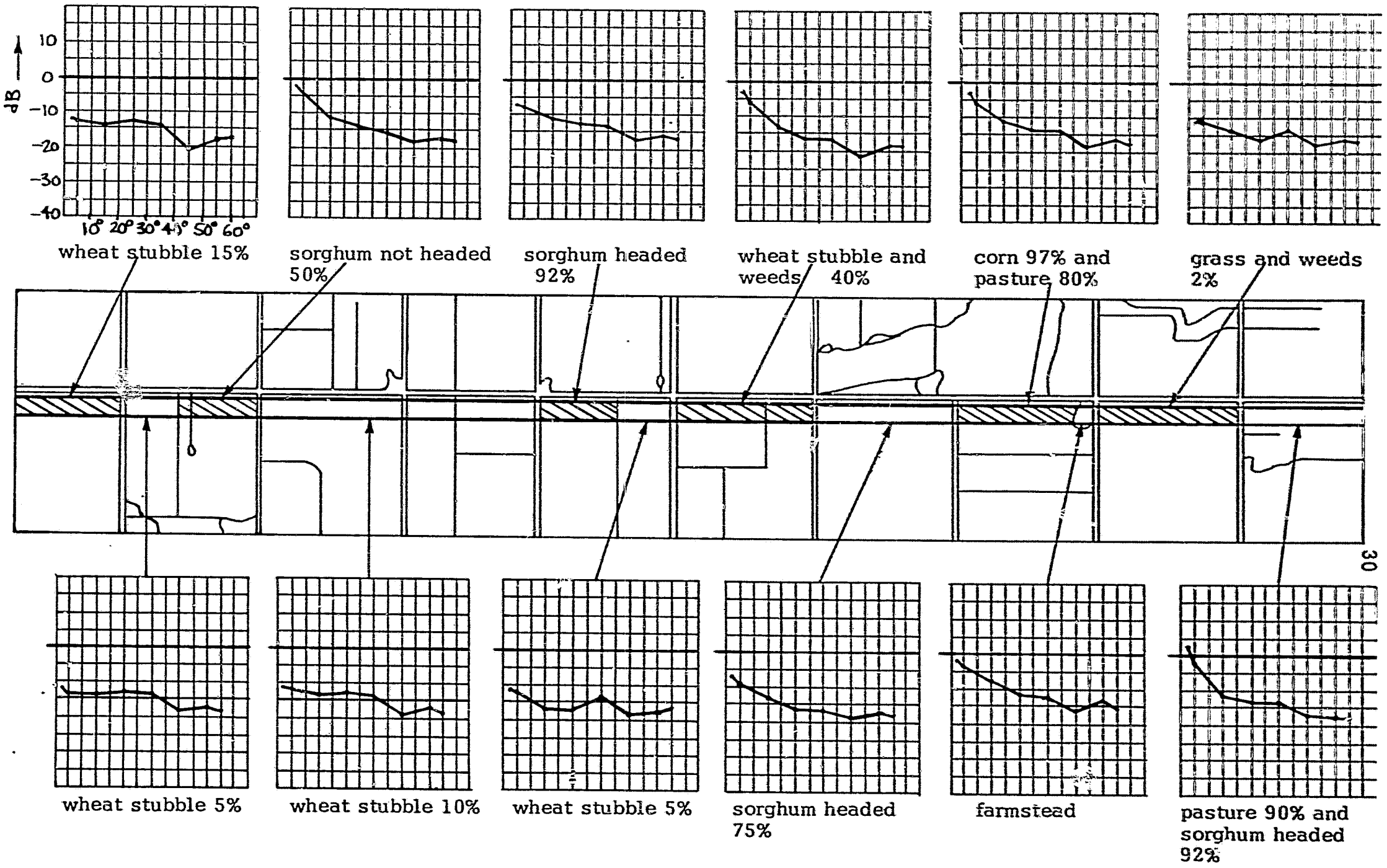

Figure 12(b). AVERAGE SCATTEROMETRY σ° (IN DB) FOR EACH CONTINUOUS AND HOMOGENEOUS FIELD VERSUS FORE INCIDENCE ANGLE (Θ) FOR FLIGHT1, LINE 1, RUN 1, MISSION 32, SITE 76, (GARDEN CITY, KANSAS), MILES' 9, 10, 11, 12, AND 13, 9-19-1966.

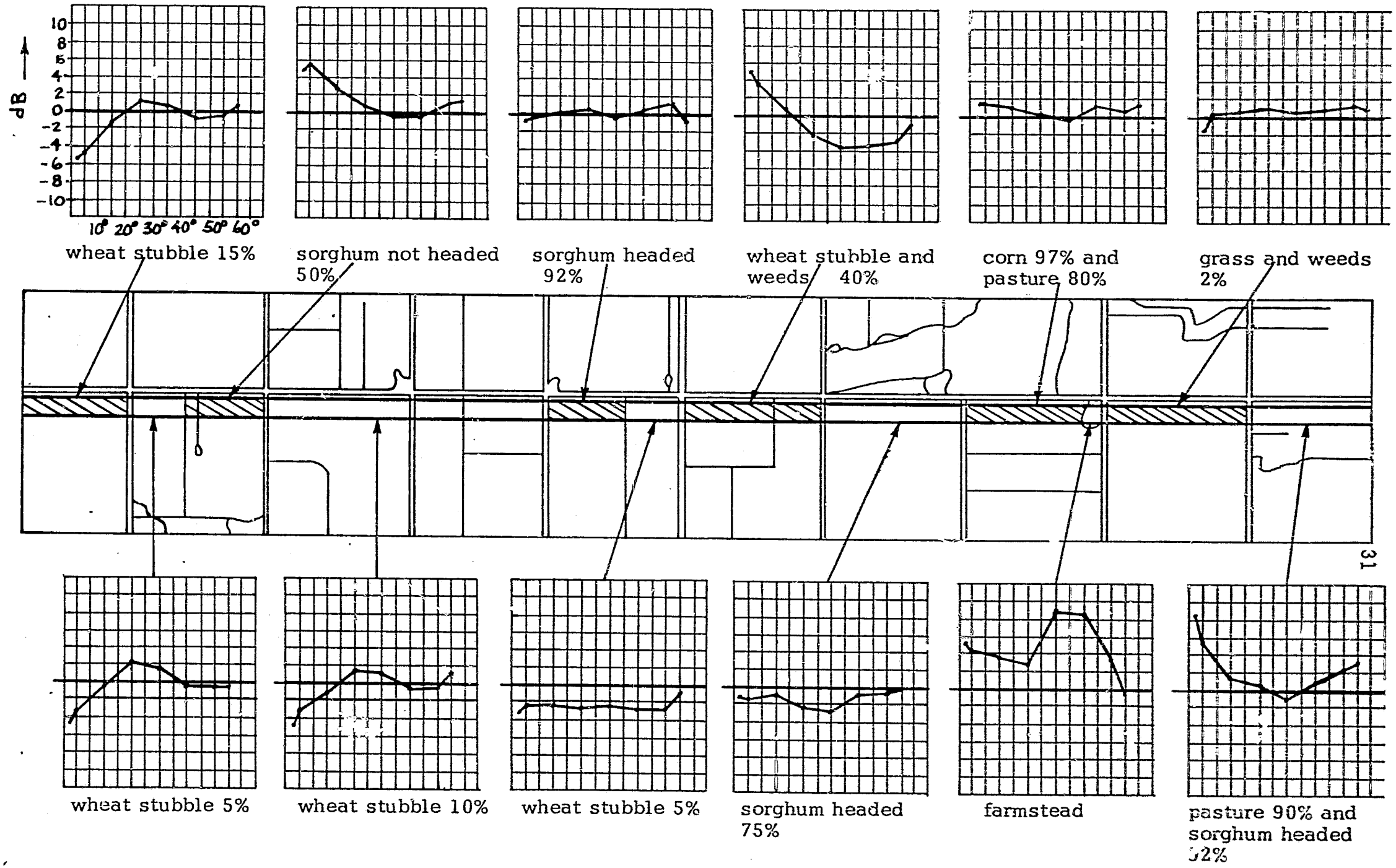

Figure 13(a). DEVIATION FROM AVERAGE RETURN CURVE VS AFT ANGLE CURVES FOR FLIGHT 1, LINE1, RUN 1, MISSION 32, SITE 76, (GARDEN CITY, KANSAS), MILES' 9, 10, 11, 12, AND 13, 9-19-1966.

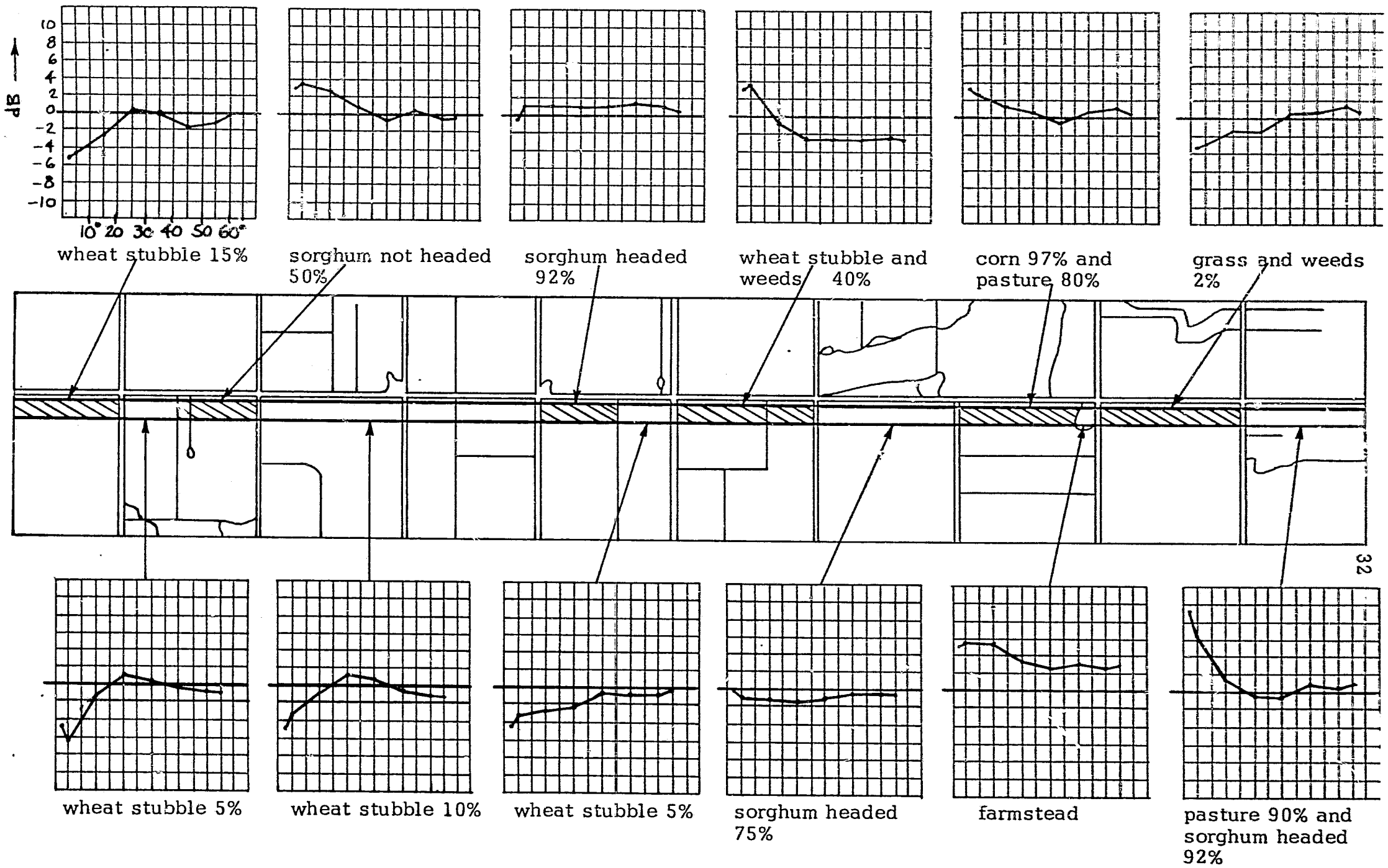

Figure 13(b). DEVIATION FROM AVERAGE RETURN CURVE VS FORE ANGLE CURVES FOR FLIGHT 1, LINE 1, RUN 1, MISSION 32, SITE 76, (GARDEN CITY, KANSAS), MILES' 9, 10, 11, 12, AND 13, 9-19-1966.

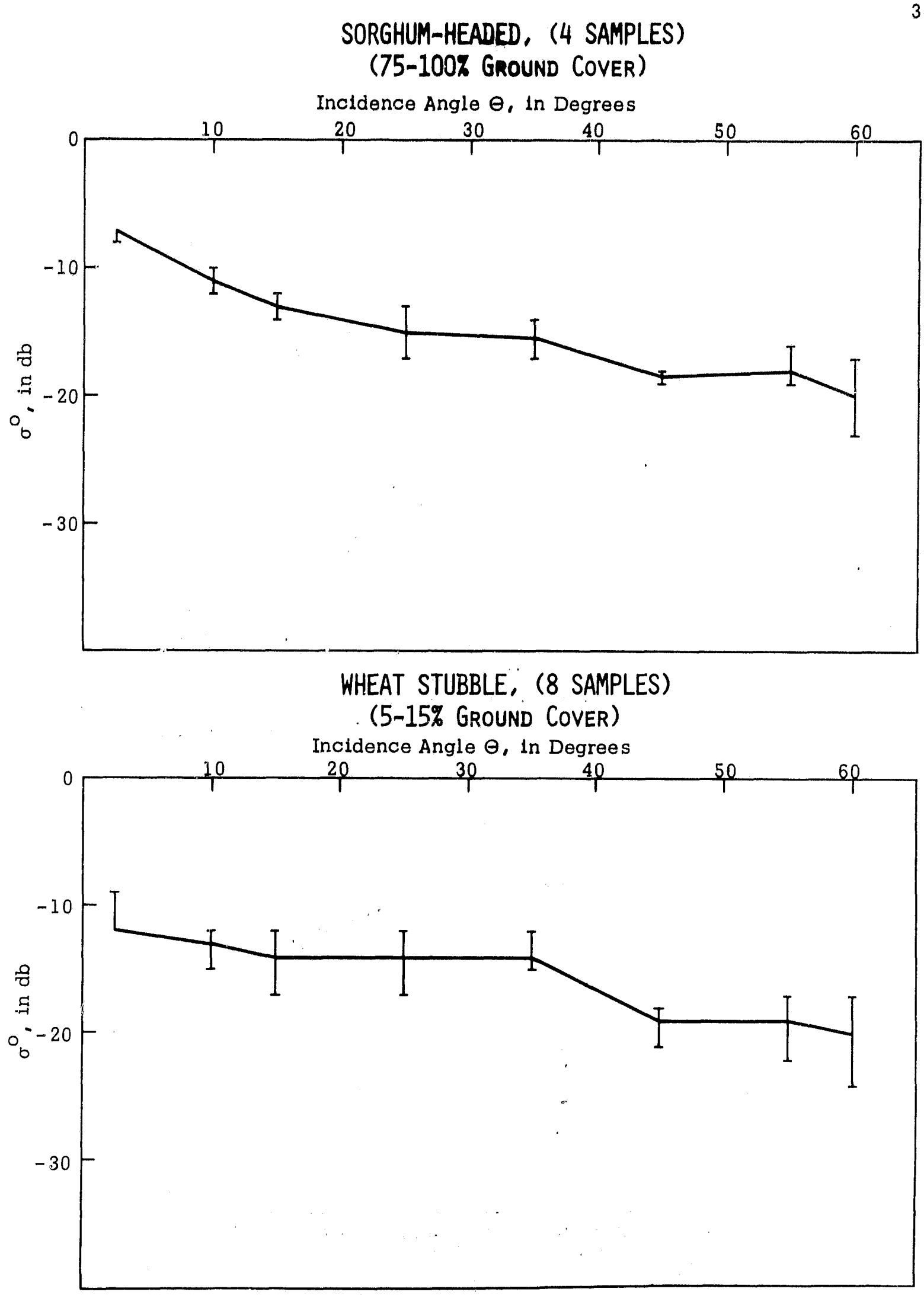

Figure 13(c): Average Scatterometry Signature for Mission 32. Limits are the Upper and Lower variation of σ^{o}.

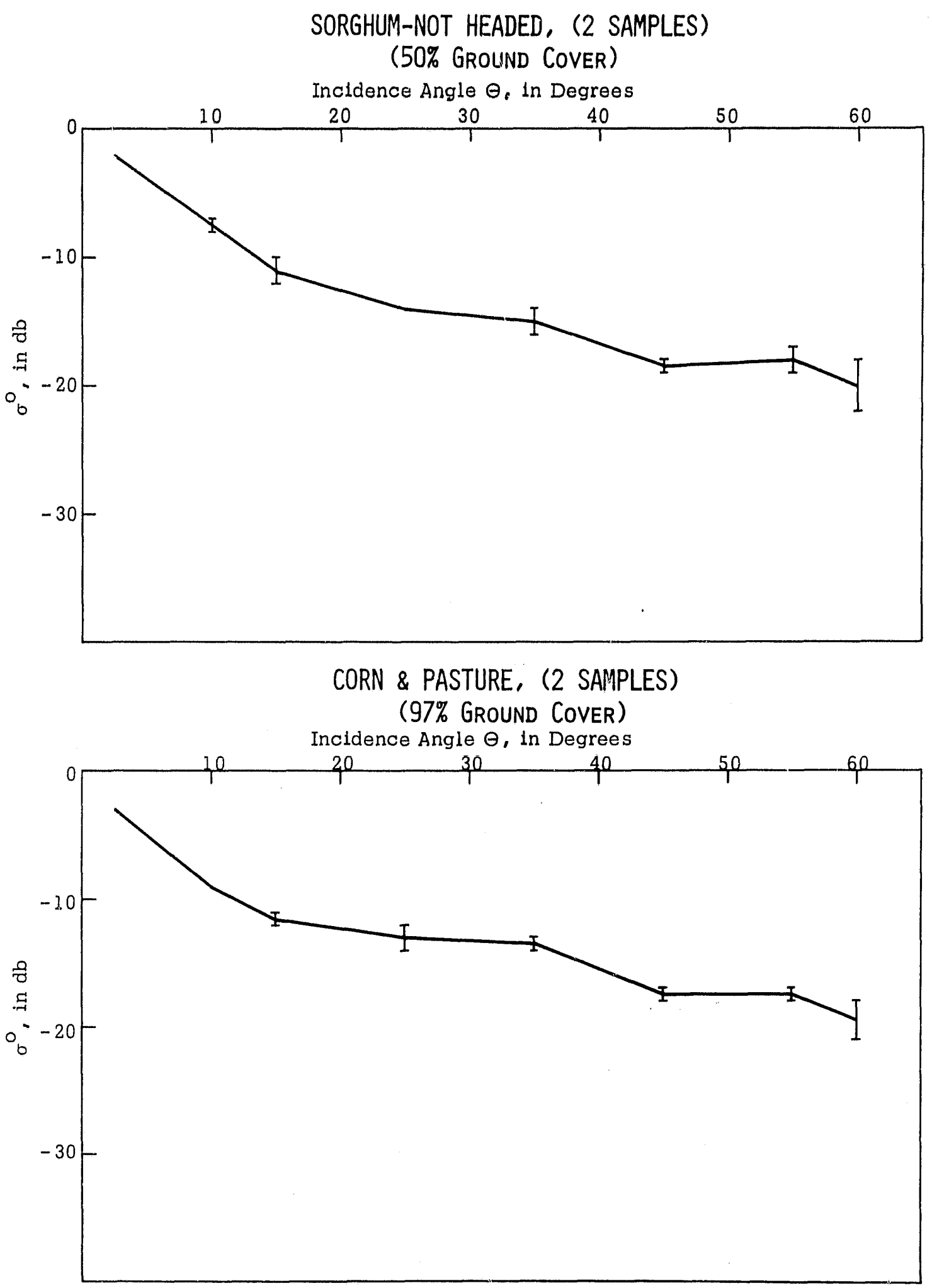

Figure 13(d): Average Scatterometry Signature for Mission 32. Limits are the Upper and Lower Variation of σ^{o}.

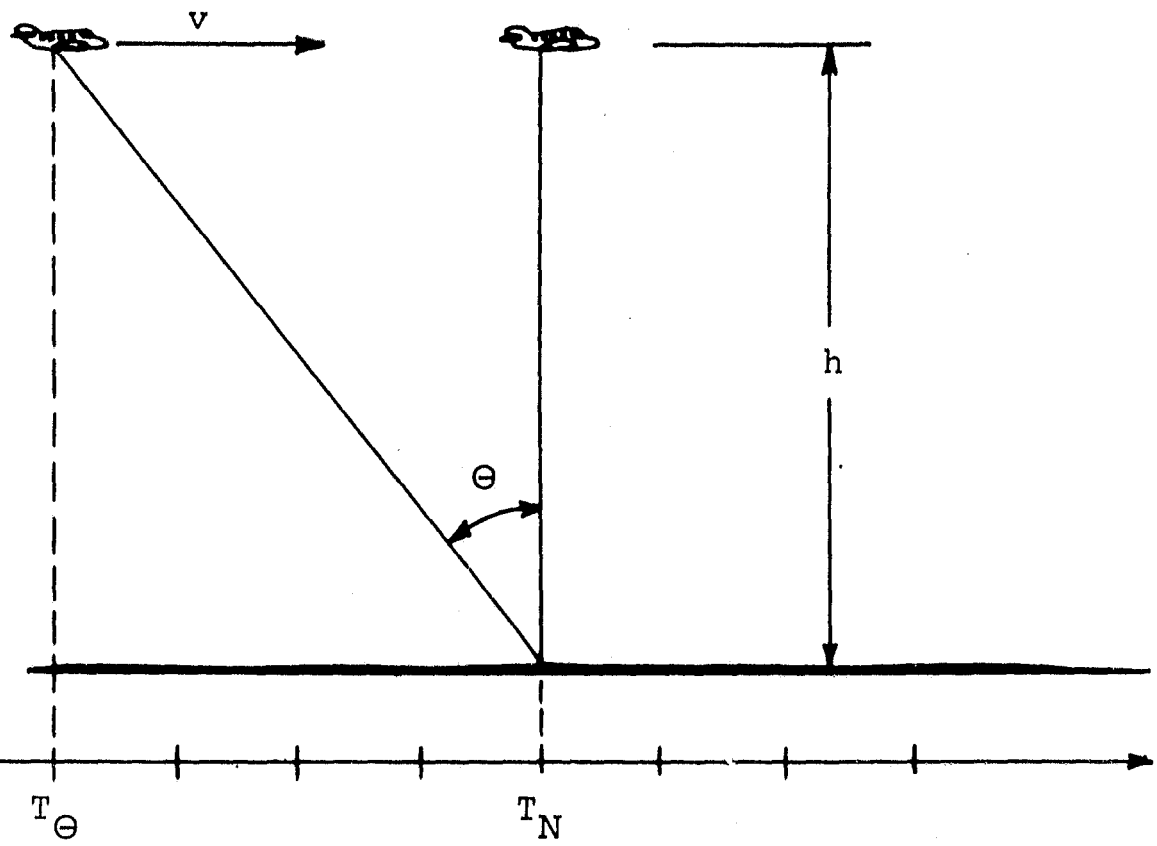

$$(T_N - T_\Theta)v = h \tan \Theta$$

$$T_N = T_\Theta + h \tan \Theta / v$$

Figure 14. DATA TIME VERSUS AIRCRAFT POSITION AND VELOCITY.

TABLE 1

CORRELATION OF AERIAL PHOTOGRAPH TIME WITH CONTROL PANEL TIME

AERIAL PHOTO TIME	CONTROL PANEL TIME	AERIAL PHOTO TIME	CONTROL PANEL TIME	AERIAL PHOTO TIME	CONTROL PANEL TIME
---- --	14:17 45	2:19 15	14:21 29	2:21 17	14:23 31
---- --	14:17 45	2:19 21	14:21 35	2:21 24	14:23 37
---- --	14:19 40	2:19 28	14:21 42	2:21 30	14:23 44
---- --	14:19 40	2:19 35	14:21 48	2:21 36	14:23 50
2:17 31	14:19 46	2:19 40	14:21 54	2:21 43	14:23 56
2:17 38	14:19 52	2:19 47	14:22 01	2:21 49	14:24 03
2:17 45	14:19 59	2:19 54	14:22 07	2:21 55	14:24 09
2:17 51	14:20 05	2:20 00	14:22 14	2:22 02	14:24 16
2:17 58	14:20 12	2:20 06	14:22 20	2:22 09	14:24 22
2:18 05	14:20 18	2:20 13	14:22 27	2:22 15	14:24 29
2:18 17	14:20 31	2:20 20	14:22 33	2:22 21	14:24 35
2:18 24	14:20 37	2:20 25	14:22 39	2:22 28	14:24 42
2:18 30	14:20 44	2:20 32	14:22 46	2:22 35	14:24 48
2:18 36	14:20 50	2:20 39	14:22 52	2:22 40	14:24 54
2:18 43	14:20 56	2:20 45	14:22 59	2:22 50	14:25 03
2:18 50	14:21 03	2:20 51	14:23 05	2:22 55	14:25 10
2:18 55	14:21 09	2:20 58	14:23 13	2:23 02	14:25 16
2:19 02	14:21 16	2:21 04	14:23 18	2:23 09	14:25 23
2:19 08	14:21 22	2:21 10	14:23 24	2:23 15	14:25 29

Data From: Flight Line 1, Run 1, Mission 32
Site 76, Garden City, Kansas
September 9, 1966

TABLE 2(a)

SEGMENT OF SCATTEROMETER COEFFICIENTS

Sigma vs Theta, in db

AFT INCIDENT ANGLE

Resolution Cell Number	2.5°	5°	15°	25°	35°	45°	55°	60°
540	-11.07	-11.94	-13.35	-11.54	-13.04	-19.51	-20.94	-22.20
550	-11.08	-11.24	-13.12	-12.34	-11.01	-17.76	-19.70	-22.46
560	- 0.36	- 1.37	-11.23	-14.21	-14.43	-18.33	-19.39	-23.13
570	-11.58	-10.45	-13.24	-13.69	-11.49	-18.99	-19.77	-19.86
580	-10.84	-11.09	-11.57	-11.76	-11.86	-18.16	-17.65	-22.07
590	-10.82	-11.28	-13.53	-13.58	-12.51	-19.20	-19.14	-19.25
600	- 7.15	- 8.22	-11.55	-13.30	-13.60	-17.15	-21.15	-23.98
610	- 7.96	- 7.47	-12.31	-15.54	-14.01	-20.59	-22.07	-21.69
620	- 2.03	- 3.00	-11.51	-17.02	-17.59	-22.33	-21.86	-24.82
630	- 8.04	- 9.21	-11.97	-15.61	-15.99	-21.29	-19.42	-23.03
640	- 8.65	- 9.68	-13.58	-16.46	-15.19	-19.13	-20.41	-23.34
650	- 3.35	- 6.44	-10.97	-13.86	-13.63	-17.76	-17.76	-20.92
660	- 8.92	- 9.41	-12.25	-14.30	-12.41	-17.93	-15.57	-24.20
670	-11.00	-11.70	-14.41	-15.91	-15.20	-19.79	-20.57	-24.48
680	2.24	- 2.26	- 9.95	-13.85	-14.78	-17.93	-19.30	-18.47

TABLE 2(b)

CORRELATION OF RESOLUTION CELL NUMBER WITH CONTROL PANEL TIME

RESOLUTION CELL NUMBER	TIME AIRCRAFT ABOVE CELL (T_N)	
540	14:23	25.48
545		28.64
550		31.81
555		34.97
560		38.14
565		41.30
570		44.47
575		47.63
580		50.79
585		53.96
590		57.12
595	14:24	0.29
600		3.45
605		6.62
610		9.78
615		12.95
620		16.11
625		19.28
630		22.44
635		25.60
640		28.77
645		31.93
650		35.10
655		38.26
660		41.43
665		44.59
670		47.76
675		50.92
680		54.08
685		57.25
690	14:25	0.41
695		3.58

TABLE 3

IDENTIFICATION OF GROUND TERRAIN

RESOLUTION CELL NUMBERS		AGRICULTURAL CLASSIFICATION
Fore	Aft	
498-512	532-546	Wheat Stubble 15 per cent Coverage
513-518	547-552	Wheat Stubble 5 per cent Coverage
519-529	553-563	Sorghum not headed 50 per cent Coverage
530-560	564-594	Wheat Stubble 10 per cent Coverage
561-570	595-604	Sorghum headed 92 per cent Coverage
571-576	605-610	Wheat Stubble 5 per cent Coverage
577-593	611-627	Wheat Subble and Weeds 40 per cent Coverage
594-609	628-643	Sorghum headed 75 per cent Coverage
610-622	644-656	Corn 97 per cent Coverage and Adjacent Pasture 80 per cent Coverage
623-625	657-659	Farmstead
626- 641	660-675	Grass and Weeds 2 per cent Coverage
642-656	676-690	Pasture 90 per cent Coverage and Adjacent Sorghum Headed 92 per cent.